CHAPTER 4

PHASE TRANSITIONS IN FRUSTRATED VECTOR SPIN SYSTEMS: NUMERICAL STUDIES

Damien Loison
Institut für Theoretische Physik, Freie Universität Berlin, Arnimallee 14, 14195 Berlin, Germany
Damien.Loison@physik.fu-berlin.de

Abbreviations

Some abbreviations are used in this chapter (by alphabetic order):
bct=body-centered-tetragonal,
BS=Breakdown of Symmetry, d=dimension, fcc=face-centered cubic lattice, FSS=Finite Size Scaling, GS=Ground State, hcp=hexagonal-close-packed lattice, KT=Kosterlitz-Thouless, L=system size, MC=Monte Carlo, MCRG=Monte Carlo Renormalization Group, N= number of components of the spin $\mathbf{S}$, NN=Nearest Neighbors, NNN=Next Nearest Neighbors, RG=Renormalization Group, STA=Stacked Triangular Antiferromagnetic lattices, STAR=Stacked Triangular Antiferromagnetic lattices with Rigidity, T=Temperature, T_c=critical Temperature, $V_{N,P}$=Stiefel model.

1. Introduction

We present in this chapter a review on recent numerical studies dealing with frustrated vector spin systems in two and three dimensions. A system of spins is frustrated when all interactions between spin pairs cannot have simultaneously their optimal values. In other words a system is frustrated when the global order is incompatible with the local one, a definition applicable in a broader sense and not restricted to spins. For spin systems frustration has the consequence that the ordered state is different from the collinear order found for common unfrustrated antiferromagnets or ferromagnets. To study and to classify the phase transitions between the ordered

and less ordered states the symmetries these states play an important role. The critical behavior of second order transitions is principally governed by the change of symmetries. Therefore even very different systems like superfluid helium and XY spin systems can have the same critical properties. This fact is called universality and our objective is to analyze the corresponding universality classes for frustrated spin systems. We will mainly review magnetic models since they are the easiest to analyze numerically and theoretically. Nevertheless the results should be valid for any system belonging to the same universality class.

During the last decade important progress has been made in the understanding of the physics of frustrated spin systems. For example there is now convincing evidence on the genuine first order nature of the phase transition for XY and Heisenberg spins for the three dimensional Stacked Triangular Antiferromagnet (STA). This still contradicts the latest renormalization group expansion based on resummation. We think that studying phase transitions of vector spins theoretically, numerically and experimentally should have implications beyond this special field, that is for the understanding and the theory of phase transition in general.

We will concentrate our attention to the phase transition of the physical XY and Heisenberg spin systems in two and three dimensions. However, to understand these systems we have to analyze also the phase transitions of frustrated spins of N components, where N takes all integer values from 1 to ∞ and not only 2 and 3 for XY and Heisenberg spins. We will also present studies for dimension d varying between two and four. Then we will review the particular case of strictly two dimensions where topological defects have a dominant role.

Frustrated Ising models are reviewed also in this book by Diep and Giacomini (chapter 1) and by Nagai, Horiguchi and Miyashita (chapter 2).

Since most of numerical simulations presented here use the Monte Carlo method, a short appendix (6) at the end is devoted to this technique. In addition, since the renormalization group is fundamental to the understanding of phase transitions, a small appendix (6) is added to discuss the methods used here for frustrated spin systems.

2. Breakdown of Symmetry

We first briefly review the fundamental concept of the reduction or the Breakdown of Symmetry (BS) in the transition from the high- to the low-temperature phases. The classification of phase transitions in universality

classes is based on this concept.

2.1. *Symmetry in the high-temperature region*

We will consider the Hamiltonian:

$$H = -J_1 \sum_{(ij)} \mathbf{S}_i.\mathbf{S}_j \tag{1}$$

where $\mathbf{S}_i$ are N component classical vectors of unit length and the sum is usually restricted to the nearest neighbors or at least to short range interactions. The symmetry of this Hamiltonian is $O(N)$ or equivalently $Z_2 \otimes SO(N)$ where $O(N)$ is the orthogonal transformation group of N-dimensional Euclidean space. For $SO(N)$ the determinant is unity, and the Ising symmetry Z_2 corresponds to the mirror operation. If we add other terms, like dipolar interactions or anisotropies, the symmetry group will be reduced. Some other changes, like a cubic term $(\mathbf{S}_i.\mathbf{S}_j)^3$, will not reduce the symmetry. In many experiments anisotropies will reduce Heisenberg ($N = 3$) symmetry to XY ($N = 2$) or Ising ($N = 1$) symmetry. Long-range interactions could also be present and the interpretation of experimental results could be problematic (see the crossover section in 6).

We will also encounter the Potts symmetry Z_q. The Potts model has the Hamiltonian:

$$H = -J_1 \sum_{(ij)} \delta_{q_i q_j} \tag{2}$$

$\delta_{q_i q_j}$ refers to the q states Potts spin with $\delta_{q_i q_j} = 0$ when $q_i \neq q_j$ and $\delta_{q_i q_j} = 1$ when $q_i = q_j$.

In addition we have to consider the symmetry of the lattice which is the sum of all symmetry elements which let the lattice invariant. For example, the triangular lattice has C_{3v} symmetry and the square lattice C_4 symmetry.[1] Therefore we have to take into account the total BS composed of the $O(N)$ spin rotations and the symmetries of the lattice.

2.2. *Breakdown of symmetry for ferromagnetic systems*

If J_1 in (1) is taken positive the Ground State (GS), for any lattice, is ferromagnetic with collinear spins pointing in the same direction. If J_1 is negative (antiferromagnetic) but there is no frustration like for the square lattice, the GS is collinear with alternating direction. Then the BS will be identical to the ferromagnetic case. The symmetry at low temperature is

$O(N-1)$ for the spins and the lattice symmetries are preserved. Therefore the BS is $O(N) \longrightarrow O(N-1)$ where $O(N)$ is the symmetry of the phase at high temperatures and $O(N-1)$ the symmetry at low temperatures. We will denote this BS $O(N)/O(N-1)$. Keeping in mind that $O(0) \equiv 1$, $O(1) \equiv Z_2$, $SO(1) \equiv 1$ and $O(N) \equiv Z_2 \otimes SO(N)$ for $N \geq 2$, the BS $O(N)/O(N-1)$ can be written as Z_2 for $N = 1$, $SO(2)$ for $N = 2$, and $SO(N)/SO(N-1)$ for $N > 2$.

All the ferromagnetic systems (cubic, stacked triangular, ...) with a Hamiltonian of type (1) have an identical BS and consequently belong to the same universality class. The only relevant variables are the dimension of the spin space, i.e. the number of components of the spin N, and the dimension of the real space d.

For Potts ferromagnetic system with a Hamiltonian of the type (2) and $J_1 > 0$, the Potts symmetry is broken in the low temperatures phase and the BS is simply Z_q. Again this does not depend on details of the system. This model has a second order phase transition for $q \leq q_c$ and a first order phase transition for $q > q_c$. We know that $q_c = 4$ in two dimensions and $q_c < 3$ in three dimensions. Therefore, in three dimensions, for any $q \geq 3$ the transition will be of first order.

In Table 1 we give the value of the critical exponents calculated by the Renormalization Group[2] (RG) depending on N and q in three dimensions ($d = 3$). Even if $N > 3$ does not correspond to physical systems, we will get very useful information for frustrated systems.

Table 1. Critical exponents for the ferromagnetic systems in three dimensions calculated by RG. $^{(a)}$We cannot define exponents in a first-order transition, however in the case of a weak first-order transition the exponents found with MC and in experiments must tend to these values. $^{(b)}$calculated by $\gamma/\nu = 2 - \eta$.

BS	α	β	γ	ν	η
$O(1)/O(0) \equiv Z_2$	0.107	0.327	1.239	0.631	0.038
$O(2)/O(1) \equiv SO(2)$	-0.010	0.348	1.315	0.670	0.039
$O(3)/O(2) \equiv SO(3)/SO(2)$	-0.117	0.366	1.386	0.706	0.038
$O(4)/O(3) \equiv SO(4)/SO(3)$	-0.213	0.382	1.449	0.738	0.036
$O(6)/O(5) \equiv SO(6)/SO(5)$	-0.370	0.407	1.556	0.790	0.031
$1st$ order$^{(a)}$ (Z_q if $q > 3$)	1	0	1	1/3	-1$^{(b)}$

2.3. *Breakdown of symmetry for frustrated systems*

The BS in frustrated systems is more complicated. We will present examples where the $O(N)$ symmetry is reduced to $O(N-1)$, $O(N-2)$, $\cdots$, $O(O)$ (completely broken in the last case). In addition it is possible that the lattice symmetry is also reduced, usually giving an additional Z_q (mostly $q=2$ and $q=3$) broken symmetry. Therefore the possible BS are $S_{lattice} \otimes O(N)/O(N-P)$ with $S_{lattice} = 1$, Z_2 or Z_3 and P varies from 1 to N.

2.3.1. *Stacked triangular antiferromagnetic lattices*

We consider here the stacked triangular antiferromagnetic lattice (STA) with nearest-neighbor (NN) and next-nearest-neighbor (NNN) J_2 antiferromagnetic interactions, J_1 and J_2, respectively. There is no frustration along the z axis (the direction of stacking) and therefore the interaction can be ferromagnetic or antiferromagnetic along z. We will explain this case in detail since it shows many phenomena appearing in frustrated systems.

- **$\mathbf{J_2 = 0}$:** Consider the case without second neighbor interaction ($J_2 = 0$). It is not possible for all three spins at the corners of a triangle to have the optimal antiparallel orientation which would minimize the energy of individual pair interactions. The resulting compromise in the case of vector spins is the so–called 120° structure, as shown in Fig. 1 (see chapter 1). In frustrated systems, local minimization of the energy is not compatible with the global energy minimum (or minima). A formal definition proposed by Toulouse[3] (and also Villain[4]) in the study of spin glasses states that a geometry is frustrated if the sign of the product of exchange interactions J_i around a plaquette C

$$\Phi_C = \mathrm{sign}\Big[\prod_{i \epsilon C} J_i\Big] \tag{3}$$

  is negative (where $J_i < 0$ implies antiferromagnetic interactions). An antiferromagnetic triangular plaquette is thus frustrated as it involves a product of three $J_i < 0$. The triangular lattice is *fully frustrated* since all plaquettes satisfy this rule. The principal effect of the frustration here is that it gives rise to a non–collinear magnetic order. This spin-order GS (I) is planar and stable as long as next nearest neighbor interaction is small, that is $0 \leq J_2/J_1 \leq 0.125$.

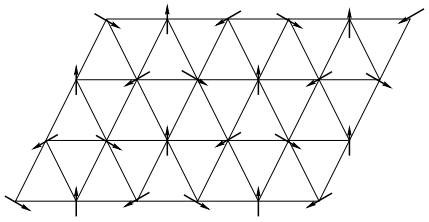

Fig. 1. Ground State I of the antiferromagnetic triangular lattice (first neighbors only). The GS has a 120° spin structure.

The BS between the disordered phase at high temperatures and the phase at low temperatures is $O(N)/O(N-2)$ which is equivalent to $Z_2 \otimes SO(2)$ for $N = 2$ and $SO(N)/SO(N-2)$ for $N > 2$. We notice that the exact value of the angle between the spin directions plays no role for the phase transition.

This system has been extensively studied in three dimensions for XY spins[5,6,7,8,9] for Heisenberg spin,[5,8,10,11,12] and for the unphysical systems $N = 6$ in Ref. [13] and $N = 8$ in Ref. [8]. The two dimensional systems have also been the subject of several studies for XY spins[107,108,109,110,111] and also for Heisenberg spins.[146]

- **$0.125 \leq J_2/J_1 \leq 1$:** Consider the presence of an antiferromagnetic second neighbor interactions (J_2) in the xy plane. The GS can be determined by minimizing the energy after a Fourier transform.[14] For $0 \leq J_2/J_1 \leq 0.125$, the GS is still the 120° structure. For $0.125 \leq J_2/J_1 \leq 1$ the GS is degenerate with θ taking any value between 0 and 2π (see Fig. 2). However the degeneracy will be lifted by thermal fluctuations (spin waves) and only a collinear GS (II) will be chosen.[15] This phenomenon, called "order by disorder" following Villain,[16] is general in frustrated systems and we will see other examples (fcc, hcp) later. There are three ways to choose the parallel spins and the BS of the lattice symmetry C_{3v} is a three-state Potts symmetry Z_3. The total BS is $Z_3 \otimes O(N)/O(N-1)$. For XY spins ($N = 2$) it is equivalent to $Z_3 \otimes SO(2)$, and to $Z_3 \otimes SO(N)/SO(N-1)$ for $N > 2$.

  Numerical studies have been done for the three-dimensional case by Loison, Diep and Boubcheur.[7,11]
- $J_2/J_1 > 1$: Now consider that $J_2/J_1 > 1$. The ground state is also degenerate, but this degeneracy is lifted by thermal fluctuations.

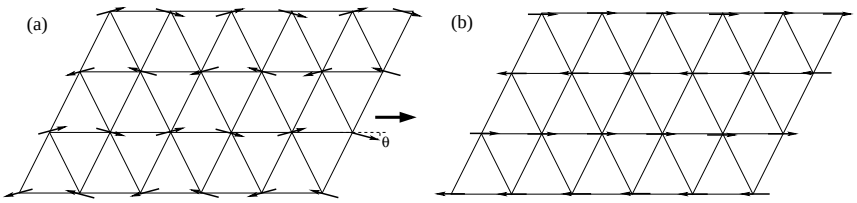

Fig. 2. Ground State (II) of the antiferromagnetic triangular lattice with first (J_1) and second (J_2)-neighbor antiferromagnetic interactions. $0.125 \leq J_2/J_1 \leq 1$. (a) θ can take any value between 0 and 2π. (b) at $T > 0$ only the "most collinear" GS is chosen.

The GS (III) is no more collinear, but still planar (see Fig. 3) and there is still three ways to choose the parallel spins. α is determined by $\cos(\alpha) = -0.5 \cdot (1 + J_1/J_2)$ and can be incommensurable, i.e. does not correspond to a rational value. Furthermore α varies slowly as a function of the temperature. The BS is $Z_3 \otimes O(N)/O(N-2)$ which is equivalent to $Z_3 \otimes Z_2 \otimes SO(2)$ for $N = 2$ (XY spins), to $Z_3 \otimes SO(3)$ for $N = 3$ (Heisenberg spins), and to $Z_3 \otimes SO(N)/SO(N-2)$ if $N \geq 4$. Numerically the incommensurable angle is problematic. Indeed we have to impose periodic boundary conditions and since α varies with the temperature, the size chosen compatible with $\alpha(T = 0)$ is no more compatible with $\alpha(T > 0) < \alpha(T = 0)$ for higher temperatures. Therefore the use of Finite Size Scaling technique (FSS, see 6) to calculate the critical exponents will be problematic.[17] In addition the GS III may not be stable under the new boundary constraint. Then the Potts symmetry could not be broken and the BS could be just $O(N)/O(N-2)$, and does not belong to the same universality class as previously. We will have an akin problem for helimagnets (see later) and for triangular lattices with two distinct nearest-neighbor interactions.[17,18]

This model has been studied in three dimensions by Loison, Diep and Boubcheur.[7,11]

- **Other BS:** We have seen the three BS which appear between the disordered phase and the GS. In addition two other transitions appear for a small range of J_2/J_1 near 0.125 and 1: between the GS I and II for $0.120 < J_2/J_1 \leq 0.125$, and between the GS II and III for $1 \leq J_2/J_1 < 1.05$.[7,11] This is a general scheme: due to thermal fluctuation the most collinear state is favored when the temperature increases. Looking at the symmetries we can get the

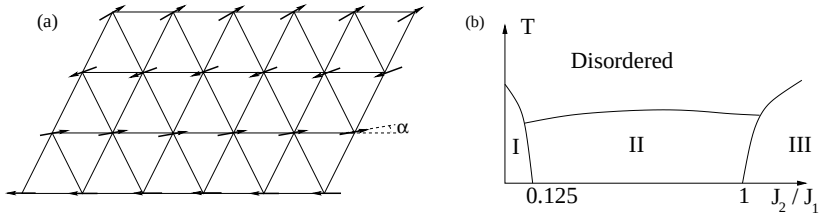

Fig. 3. (a) Ground State III of the antiferromagnetic triangular lattice with first (J_1) and second (J_2) -neighbor antiferromagnetic interactions. $1 < J_2/J_1$. (b) Phase diagram in the $(J_2/J_1, T)$ space.

order and even the universality class of these transitions.
The GS III and II are compatible in the sense that at the transition α will go smoothly to zero and the transition could be of second order. The BS between III and II is $O(N-1)/O(N-2)$ and consequently the transition should be $N-1$ ferromagnetic type.
The GS I and II are incompatible because there is no way to go smoothly from one to the other and the transition should be of first order.

2.3.2. *bct Helimagnets*

We consider the body–centered–tetragonal (bct) helimagnets. The competition between the J_1 and J_2 interactions gives rise to a helical ordering along the z axis (see Fig. 4). This GS is characterized by the turn angle α between spins belonging to two adjacent planes perpendicular to the z axis. α is given by the formula $\cos(\alpha) = -J_2/J_1$ and α decreases slowly as function of the temperature. There is no breakdown of the symmetry of the lattice, the GS is non collinear but planar and the BS is $O(N)/O(N-2)$, i.e. identical as the STA with first nearest neighbor interaction only.

Numerically we have a similar problem as for the STA with large NNN interaction: $\alpha(T)$ varies as a function of the temperature, but with periodic boundary conditions a constraint is present.

Nevertheless effect of this constraint should not be too strong. Indeed a small constraint will not break a symmetry of the lattice and for the XY, it will not change the BS of the spin rotation because all the symmetries of the rotation group are already broken. For Heisenberg spins the GS could become non coplanar, but this is unlikely. Therefore we should find the same universality as that of the STA. The only difference will be a new

correction to the scaling laws for a second order phase transition. But for a first order one the boundary conditions would not matter.

This model has been studied by Diep and Loison[19,20]. A quantum version has also been considered by Quartu and Diep [21].

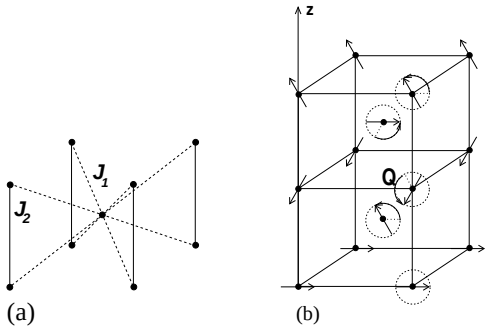

Fig. 4. a. Interactions for the bct. b. Ground State for the bct for $J_2/J_1 = 0.5$.

2.3.3. *Stacked J_1–J_2 square lattices*

The J_1–J_2 simple cubic lattice is made by stacking along the z axis the square lattices with antiferromagnetic (or ferromagnetic) first nearest neighbor interaction (J_1) and antiferromagnetic second nearest neighbor interaction (J_2) in the xy plane. For $J_2/J_1 > 0.5$ the GS is degenerate but by "order by disorder" only collinear configurations appear (see Fig. 5). There are two ways to place the parallel spins (following the x or y axis) and a Z_2 Ising symmetry of the lattice symmetry is broken. The BS will be $Z_2 * O(N)/O(N-1)$ or equivalently $Z_2 \otimes SO(2)$ for $N = 2$ and $Z_2 \otimes SO(N)/SO(N-1)$ for $N > 2$. For XY spins, there exists an identical BS as for the STA with first nearest neighbor interaction only. Therefore the two systems for $N = 2$ should belong to the same universality class.

No numerical studies have been done on this model for the three-dimensional case. The two-dimensional case has been studied by Loison and Simon.[22]

2.3.4. *The simple cubic J_1–J_2 lattice*

The simple cubic J_1–J_2 lattice is similar to the stacked J_1–J_2 square lattices shown above, but the second neighbor interactions are also present in the

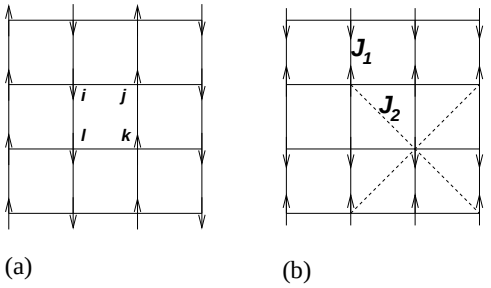

Fig. 5. Ground State of the stacked J_1–J_2 lattice with first (J_1) and second (J_2) - neighbor antiferromagnetic interactions. $J_2/J_1 > 0.5$. (a) and (b) show the two possible configurations at non zero temperature.

xz and yz planes. Similarly, by "order by disorder" the spin configuration is collinear, but now there are three ways to choose the direction of parallel spins (the z axis in addition to the x and y axes). Therefore the BS is $Z_3 \otimes O(N)/O(N-1) \equiv Z_3 \otimes SO(N)/SO(N-1)$. It is equivalent to the BS of the STA with intermediate NNN interaction.

This model has been studied for Heisenberg spin by Alonso et al,[25] and Pinettes and Diep[26].

2.3.5. J_1–J_2–J_3 *lattice*

The addition of a third-neighbor antiferromagnetic interaction to the previous model leads to new GS and therefore to a new BS. For some value of the interactions a non planar GS state appears.[27] In addition a Z_2 symmetry is broken from the lattice group and the BS is hence $Z_2 \otimes O(N)/O(N-2)$ between the ordered phase and the disordered phase. For XY spins the BS is equivalently $Z_2 \otimes Z_2 \otimes SO(2)$, and for Heisenberg spins $Z_2 \otimes SO(3)$. There exist also various transitions between various phases, but following the discussion at the end of section 2.3.1 concerning STA with NNN interaction, it is not difficult to find that the transition will be of first order or of the ferromagnetic type $SO(N-1)/SO(N-2)$.

No numerical studies have been done so far on this model.

2.3.6. *Villain lattice and fully frustrated simple cubic lattice*

The fully frustrated square lattice, called Villain lattice, is shown in Fig. 6a. This two-dimensional lattice has been extensively studied[4,107,112,113,114,115,116,117,118,119,123].

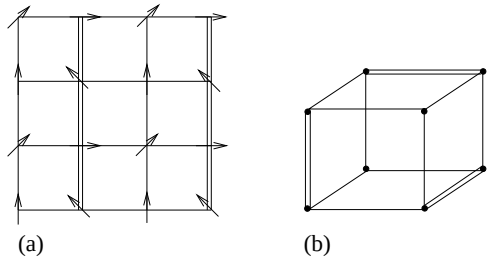

Fig. 6. a. Ground state of the stacked Villain lattice. The double lines are antiferromagnetic interactions. b. The fully frustrated cubic lattice.

The fully frustrated simple cubic lattice is made from the Villain lattice in three dimensions (see Fig. 6b). The lattice has three ferromagnetic interactions and one antiferromagnetic one for each plaquette. In this case the GS has an infinite degeneracy for Heisenberg spins and is twelve-fold degenerate for XY spins. Diep et al[23,24] and Alonso et al[25] have studied this model.

2.3.7. *Face-centered cubic lattice (fcc)*

The face-centered cubic lattice (fcc) has a degenerate GS. But like the STA with NNN interaction, the "most collinear phase" is selected by thermal fluctuations. If we consider the smaller unit tetrahedral cell (see Fig. 7), the GS consists of two parallel and two antiparallel spin pairs. There are three ways to construct. This is equivalent to a Potts Z_3 symmetry. Therefore, since the GS is collinear, the BS will be $Z_3 \otimes O(N)/O(N-1)$ or, equivalently, $Z_3 \otimes SO(N)/SO(N-1)$. This BS is identical to the STA with intermediate NNN interaction.

This model has been studied by Diep and Kawamura[28] and Alonso et al.[25]

2.3.8. *Hexagonal–close–packed lattice (hcp)*

The hexagonal–close–packed lattice (hcp) has many common features with the fcc. It is constructed by stacking tetrahedra (see Fig. 7) and an "order by disorder" mechanism lifts one part of the degeneracy of the GS resulting in a collinear GS composed with two parallel and two antiparallel spins. Equivalently to the fcc case, the BS will be $Z_3 \otimes O(N)/O(N-1)$ or equivalently $Z_3 \otimes SO(N)/SO(N-1)$. This BS is identical to the STA with

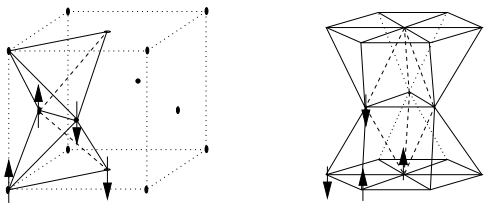

Fig. 7. a. Ground State of the fcc lattice. b. Ground State of the hcp lattice.

intermediate NNN interaction.

This model has been studied by Diep[29]

2.3.9. *Pyrochlores*

The pyrochlore lattice can be made by stacking Kagomé lattices along (111) direction and is composed of an arrangement of corner-sharing tetrahedra (see the chapters by Bramwell et al, and by Gaulin and Gardner, this book). In presence of the first and third nearest neighbor interactions Reimers[30] has proved that the GS is collinear. Similar to the fcc and hcp cases, there are three ways to place the spins on each tetrahedron. The BS should therefore be $Z_3 \otimes O(N)/O(N-1)$ or equivalently $Z_3 \otimes SO(N)/SO(N-1)$. This BS is identical to the STA with intermediate NNN interaction.

Reimers et al.[30] have studied this model.

2.3.10. *Other lattices*

We could stack a Zig–Zag model[31] and various phases and phase transitions should appear. With an equivalent analysis described at the end of the section 2.3.1 concerning STA with NNN interaction, it is not difficult to find the nature of the transitions. Still, other lattices can be considered, however as shown later, they will have equivalent BS.

2.3.11. *STAR lattices*

In addition one can construct spin systems having an identical breakdown of symmetry even if they do not correspond to a real system.

The first example is derived from the STA. Following the chapter of Delamotte et al. in this book [32] certain modes are irrelevant near the critical

point. In particular we can construct cells of three spins which are always in the ground state 120° configuration. One gets a system of cells in interaction but with a rigidity imposed inside the cells (see Fig. 8). We call this system STAR (Stacked Triangular Antiferromagnetic with Rigidity). The BS is then $O(N)/O(N-2)$, identical to STA with NN interaction.

This model has been studied in three dimensions by Dobry and Diep[33] and by Loison and Schotte.[34,35,36]

2.3.12. *Dihedral lattices $V_{N,2}$*

The second example is derived from the STAR. It is composed of two vector spins $\mathbf{e}_1$ and $\mathbf{e}_2$ constrained to be orthogonal to each other at each lattice site. The interactions are set to be ferromagnetic and the spin $\mathbf{e}_1$ ($\mathbf{e}_2$) interacts only with the other spins $\mathbf{e}_1$ ($\mathbf{e}_2$) at other sites (see the Fig. 8). This model is referred to as the dihedral model $V_{N,2}$. We note that for XY spins $N = 2$ the model can be right–handed or left–handed.

The Hamiltonian is defined by

$$H = J \sum_{<ij>} \sum_{k=1}^{P} \Big[\, \mathbf{e}_k(i) \cdot \mathbf{e}_k(j) \, \Big] \tag{4}$$

where $P = 2$.

At high temperatures the symmetry is $O(N)$ for the first vector and $O(N-1)$ for the second one, since the two vectors must be orthogonal. At low temperatures the symmetry is $O(N-1)$ for the first vector and $O(N-2)$ for the second one for the same reason. Therefore the BS is $O(N)/O(N-2)$, identical to the STA with NN interaction.

This model has been studied in three dimensions by Kunz and Zumbach[37] and by Loison and Schotte[34,35], and in two dimensions for XY spins by Nightingale, Granato, Lee, and Kosterlitz.[121,122]

2.3.13. *Right–handed trihedral lattices $V_{3,3}$*

For Heisenberg spins one can construct another model from the dihedral $V_{3,2}$ with an identical BS. By adding a third vector $\mathbf{e}_3 = \mathbf{e}_1 \times \mathbf{e}_2$ to the dihedral model no degree of freedom is added. Therefore the BS is unchanged and identical to the dihedral $V_{3,2}$ and to the STA with NN interaction, $O(3)/O(1) \equiv SO(3)$.

This model has been studied in three dimensions by Loison and Diep.[38]

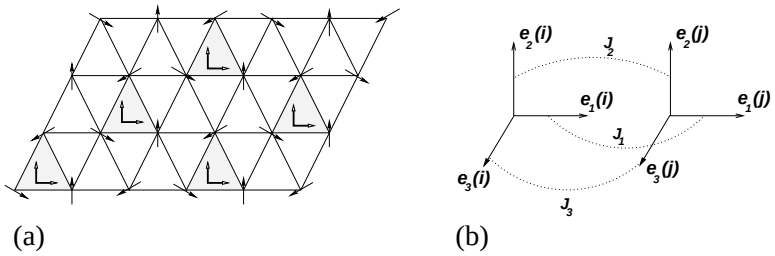

Fig. 8. a. STAR model and dihedral model. b. Trihedral model and $V_{3,P}$ model. $P = 1$ for $J_2 = J_3 = 0$, $P = 2$ for $J_3 = 0$ and $J_1 = J_2 = 1$, and $P = 3$ for $J_1 = J_2 = J_3 = 1$.

2.3.14. *P–hedral lattices* $V_{N,P}$

We can generalize the dihedral $V_{N,2}$ model to $V_{N,P}$ with P orthogonal vectors at each site. For $P = N$ the N vectors can be right- or left-handed. The BS of symmetry is then $O(N)/O(N-P)$ with $P \leq N$.

For $P = 1$ we have the ferromagnetic case, i.e. a collinear GS. For $P = 2$ we have a coplanar GS but no more collinear like in the STA with NN interaction. For $P = 3$ the GS is no more coplanar but restricted to a space in three dimensions, and so on. The case $N = P = 3$ could correspond to some experimental systems and spin glasses should also have this kind of breakdown of symmetry but in presence of disorder. For $P = N$ the BS is $O(N)/O(0) \equiv Z_2 \otimes SO(N)$.

This model has been studied by Loison.[39]

2.3.15. *Ising and Potts-*$V_{N,1}$ *model*

We define the following Hamiltonian

$$H = -J_1 \sum_{(ij)} \mathbf{S}_i.\mathbf{S}_j.\delta_{q_i q_j} \tag{5}$$

where $\mathbf{S}_i$ are N-component classical vectors of unit length, $\delta_{q_i q_j}$ are the q-state Potts spin ($q = 2$ for Ising spin) with $\delta_{q_i q_j} = 0$ when $q_i \neq q_j$, and the interaction constant J_1 is taken positive (ferromagnetic interaction). The sum runs over all nearest neighbors. For $N = 2$ this model is exactly equivalent to the dihedral $V_{2,2}$ model introduced previously.

Obviously the BS is $Z_q \otimes O(N)/O(N-1)$ or equivalently $Z_q \otimes SO(N)/SO(N-1)$ which is identical to the stacked J_1–J_2 model if $q = 2$, and to the STA with NNN interaction, fcc, hcp if $q = 3$.

This model has been studied in three dimensions by Loison.[40] and in two dimensions for XY spins by Nightingale et al.[121,122]

2.3.16. *Ising and Potts–$V_{N,2}$ model*

We can also define a dihedral model with the Hamiltonian (4) coupled with a Potts model in the same way as in (5). In this case the BS is $Z_q \otimes O(N)/O(N-2)$ which is identical to the BS for the stacked J_1–J_2–J_3 model if $q = 2$ and to the STA with a large NNN for $q = 3$.

This model has been studied by Loison.[40]

2.3.17. *Landau–Ginzburg model*

The Landau–Ginzburg Hamiltonian is constructed from the dihedral $V_{N,2}$ model (see chapter of Delamotte et al.[32]). We release the constraints on the orthogonality of the spins and on the norm unity, replacing them by a potential we arrive at the following Hamiltonian

$$H = K \sum_{<ij>} (\vec{\phi}(i) - \vec{\phi}(j))^2 + r \sum_i \vec{\phi}(i)^2 + u \sum_i \left(\vec{\phi}(i)^2\right)^2 + v \sum_i \left[(\vec{\phi}_a(i) \cdot \vec{\phi}_b(i))^2 - \vec{\phi}_a(i)^2 \vec{\phi}_b(i)^2\right] \quad (6)$$

where $\vec{\phi}(i) = \left(\vec{\phi}_a(i), \vec{\phi}_b(i)\right)$ is an $N + N$–component vector defined on the lattice site i, and the summation $\sum_{<ij>}$ runs over all nearest neighbor pairs of the lattice. The first term represents the interactions between the sites and the last term the constraint that the spins $\phi_a(i)$ and $\phi_b(i)$ are orthogonal. If $v = 0$, the Hamiltonian is reduced to a standard $O(2N)$ ferromagnetic problem. This is our third model that we call the chiral ϕ^4 model. For $v > 0$ the BS is $O(N)/O(N-2)$, identical to STA with NN interaction.

This model has been studied numerically by Itakura.[8]

2.3.18. *Cubic term in Hamiltonian*

One can introduce a model where the frustration is not geometrical but included on each link resulting in a non collinear GS. Consider the Hamiltonian for two spins:

$$H = J_1 \mathbf{S}_i.\mathbf{S}_j + J_3 (\mathbf{S}_i.\mathbf{S}_j)^3 \quad (7)$$

where $\mathbf{S}_i$ is a N component classical vector of unit length, J_1 is a ferromagnetic coupling constants $J_1 < 0$ and J_3 an antiferromagnetic one $J_3 > 0$. This cubic term has the same symmetries as the linear term and for a ferromagnetic system ($J_3 < 0$) the universality class will be identical.[41] For $1/3 \leq -J_3/J_1 \leq 4/3$ the minimum of H occurs when the two spins are canted with an angle $\cos(\alpha) = \frac{1}{\sqrt{3J_3/J_1}}$. On a cubic lattice the GS is planar, on a triangular lattice it is in three dimensions (if $N \geq 3$), on a fcc lattice it is in four dimensions (if $N \geq 4$), $\cdots$ This phase has, at finite temperature, a transition to a ferromagnetic collinear phase. Therefore the BS will be $O(N-1)/O(N-P)$ with $P = 2$ for the cubic lattice (planar GS), $P = 3$ for the stacked triangular, $P = 4$ for the fcc lattice $\cdots$ The case $P = 2$ has been tested for Heisenberg spins and it gives indeed an $O(2)/O(1) \equiv SO(2)$ transition, i.e. a ferromagnetic XY transition.[41] The case $P = 3$ has an identical BS as the STA but it has not been tested.

This model has been studied numerically by Loison.[41]

2.3.19. *Summary*

The number of models that can be constructed by adding interactions is unlimited. However, the number of BS can only be finite. As has been shown in the previous sections, the symmetry breaking is limited to $Z_q \otimes O(N)/O(N-P)$. For the physically relevant cases it is restricted to $q = 1$ (Identity), $q = 2$ (Ising), or $q = 3$ (Potts), $N = 2$ (XY spins), $N = 3$ (Heisenberg spins), and $P = 1$, 2 or 3. In total for Heisenberg spins there will exist 8 cases (two are identical: $(q = 1, P = 3) \equiv (q = 2, P = 2)$) and 5 for XY spins.

The tables below summarize the probable BS for physical frustrated systems with XY or Heisenberg spins.

3. Phase transitions between two and four dimensions: $2 < d \leq 4$

In this section we will concentrate on the nature of the various transitions mentioned in the previous section. Especially the transition for the $O(N)/O(N-2)$ BS is considered in detail since it appears in numerous systems and was extensively debated. Then we will discuss the other BS which are less problematic.

Table 2. Most probable BS for frustrated XY spin systems with corresponding lattices or models

BS	**lattice-model**
$SO(2)$	ferromagnetic, small frustration
$Z_2 \otimes SO(2)$	STA, STAR, $V_{2,2} \equiv$ Ising-$V_{2,1}$, bct, Stacked J_1–J_2, Stacked Villain, Fully Frustrated cubic, Stacked Zig-Zag, chiral ϕ^4 model, $(S_i.S_j)^3$ term
$Z_3 \otimes SO(2)$	STA+NNN, cubic J_1–J_2, fcc, hcp, pyrochlore, Potts-$V_{2,1}$
$Z_2 \otimes Z_2 \otimes SO(2)$	stacked J_1–J_2–J_3, Ising-$V_{2,2}$
$Z_3 \otimes Z_2 \otimes SO(2)$	STA+NNN, Potts-$V_{2,2}$

Table 3. Most probable BS for frustrated Heisenberg spin systems with corresponding lattices or models

BS	**lattice–model**
$SO(3)/SO(2)$	ferromagnetic, small frustration
$SO(3)$	STA, STAR, $V_{3,2}$, right–handed trihedral, bct, Stacked Villain, Stacked Zig–Zag, Fully Frustrated cubic(?), chiral ϕ^4 model, $(S_i.S_j)^3$ term
$Z_2 \otimes SO(3)/SO(2)$	Stacked J_1–J_2, Ising–$V_{3,1}$
$Z_2 \otimes SO(3)$	Stacked J_1–J_2–J_3, $V_{3,3} \equiv$Ising–$V_{3,2}$, $(S_i.S_j)^3$ term, Fully Frustrated cubic(?)
$Z_2 \otimes Z_2 \otimes SO(3)$	Ising–$V_{3,3}$
$Z_3 \otimes SO(3)/SO(2)$	STA+NNN, cubic J_1–J_2, fcc, hcp, pyrochlore, Potts–$V_{3,1}$
$Z_3 \otimes SO(3)$	STA+NNN, Potts–$V_{3,2}$
$Z_3 \otimes Z_2 \otimes SO(3)$	Potts–$V_{3,3}$

3.1. $O(N)/O(N-2)$ *breakdown of symmetry*

3.1.1. *Fixed points*

Since many models (STA, STAR, dihedral, chiral ϕ^4 model, $\cdots$, see Tables 2- 3) have an identical BS, they should have equivalent critical behavior, i.e. they belong to the same universality class. However, the situation is more complicated and even with an identical BS two systems could show different behavior. To understand this fact we have plotted in Fig. 9 the fixed points in the critical plan for this model. Since there are two fields (eq. 6) to allow coplanar non collinear GS we will have four possible fixed points.

There are two more than the ferromagnetic case which has a collinear GS and consequently only one field.

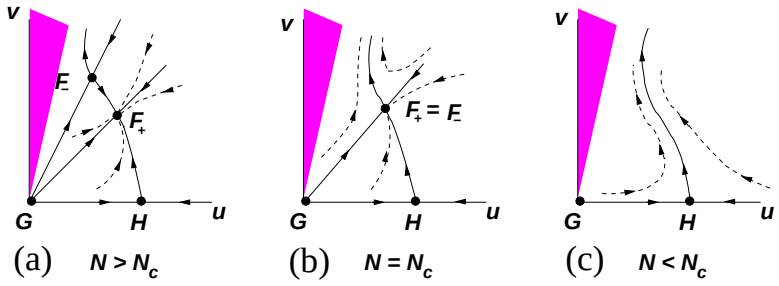

Fig. 9. (a), (b), (c) Hamiltonian flow induced by renormalization group transformations. The arrows indicate the direction of flow under iterations.

The fixed points are:

1. The Gaussian fixed G point at $u^* = v^* = 0$ with mean-field critical exponents.
2. The $O(2N)$ fixed point H at $v^* = 0$ and $u^* = u_H \neq 0$ with $O(2N)$ exponents (see Table 1).
3. Two fixed points F_+ and F_- at location (u_{F_+}, v_{F_+}) and (u_{F_-}, v_{F_-}) different from zero. These are the fixed points associated with a new universality class.

The existence and stability of the fixed points depend on the number of components N:

a. $N > N_c$: four fixed points are present but three are unstable (G, H, F_-) and a stable one F_+. Therefore the transition belongs to a new universality class different from the standard $SO(N)/SO(N-1)$ class. If the initial point for the RG flow is to the left of the line (G, F_-), see Fig. 9a, the flow is unstable and the transition will be of first order. Therefore two systems with the same Hamiltonian and the same breakdown of symmetry could have different critical behaviors.
b. $N = N_c$: the fixed points F_- and F_+ coalesce to a marginally stable fixed point. One would think that the transition is "tricritical" but the exponents are different and not given by the tricritical mean-field values contrary to common belief. The reason is that there are

two non zero quartic coupling constants, see Fig. 9b, in contrast to the "standard" tricritical point where the quartic term disappears and a sextic term takes over.

c. $N < N_c$: F$_-$ and F_+ move into the complex parameter space, see Fig. 9c. The absence of stable fixed points is interpreted as a signature of a first-order transition.

There are at least three questions: the value of N_c, the location of the initial point in the *RG* flow, and the nature of the transition.

3.1.2. *MCRG and first-order transition*

The most reliable answers to these questions can be found in the article of Itakura.[8] He studied the STA model, dihedral model, and the chiral ϕ^4 model with the Hamiltonian (6), using Monte Carlo Renormalization Group (MCRG). This method is very powerful to give the flow diagram but not the critical exponents with a great precision.

He showed that the STA and dihedral models have an initial point in the RG flow under the line GF_- in the Fig. 9. Therefore they should belong to the same universality class provided the fixed point F_+ exists, i.e. $N > N_c$. He found that N_c is between 3 and 8 in three dimensions which means that the real physical systems XY ($N = 2$) and Heisenberg spins ($N = 3$) have a first-order transition.

In addition he did a standard canonical Monte Carlo (MC) simulation for XY spins on the STA lattice for very large sizes of 96^3 and 126^3. He found a first-order transition in agreement with MCRG study, contrary to smaller size systems which seem to have a second-order transition.[5,6,7] For Heisenberg spins he could not find a first-order transition but using the results of the MCRG he concludes that the first-order transition could only be seen for a size larger than 800^3 which is not accessible for actual computer resources. For the dihedral model with a canonical MC he found a clear first-order transition for large sizes for Heisenberg spins. For XY spins Loison and Schotte have already shown that the transition is of first order. Diep[19] in 1989 was the first to find a first-order transition in helimagnetics bct lattice with XY spins. This result was considered not conclusive because of problems of periodic boundary conditions in numerical simulation. However, as noted above, this is not relevant for XY spins (contrary to Heisenberg spins) and whence this conclusion is indeed correct for this BS.

We have now to address the problem why phase transitions appear continuous for small sizes but show the true first-order nature only for larger

sizes. This phenomenon is not restricted to frustrated spin systems such as STA but appears also in the weakly first-order transition of the two-dimensional Potts model with $q = 5$ components.[42,43,44] More generally it appears when two fixed points collapse and disappears following one variable (like F_- and F_+ in Fig. 9). See later for a comparison with the Potts model.

3.1.3. *Complex fixed point or minimum in the flow*

The change from continuous to discontinuous transition can be understood using the concept of "complex fixed point" or "minimum in the flow" first introduced by Zumbach[45] and then developed by Loison and Schotte.[34,35] In Fig. 9c for $N < N_c$ the fixed points F_- and F_+ have collapsed and no solution exists in real parameter space. Instead there exists an imaginary solution plotted in Fig. 10a. These solutions should have an influence on the flow in the real plane as shown in Fig. 10b. Zumbach showed that there exists a basin of attraction due to the complex fixed points where the RG flow is very slow.

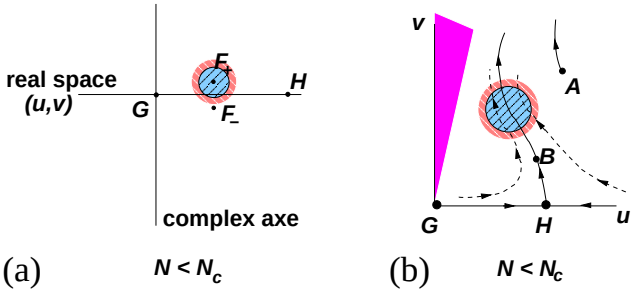

Fig. 10. a) For $N < N_c$ the fixed points F_+ and F_- become complex. b) Hypothesis on the Hamiltonian flow induced by renormalization–group transformations for $N < N_c$ (see Fig. 9c). The arrows give the direction of flow. The two circles correspond to a low velocity region. The inner one corresponds to a minimum and hence an "almost" second-order transition. The outer circle corresponds to a slow crossover where the critical exponents will vary as a function of the system size.

If the RG flow of a system goes through this region, the number of RG iterations $L \to L/b$ to get outside will be large. Therefore the size L of the numerical system considered, should be made large enough (see 6). If the size is "too small", the flow is trapped inside of this low velocity region and the transition seems to be continuous. We immediately see that the

size L for which the true first-order transition is visible, that is when the flow is outside of the basin of attraction, will depend on the starting point. If it is located outside of the domain of low velocity and if the flow does not approach this region (point A in Fig. 10), then the first-order nature of transition can be seen already for small sizes. In the other case, if the initial position is such that the flow has to go through the entire region of low velocity (point B in Fig. 10), then the necessary size to reach the true first-order region will be very large. This explains why STA, STAR, dihedral and right–handed trihedral (for $N = 3$) models having an identical breakdown of symmetry behave differently. Similarly a single system can show different behaviors for different sizes. For the Heisenberg case, for example, the right–handed trihedral model shows a strong first-order behavior even for small sizes. The dihedral model with the same BS for $N = 3$ has a weaker first-order behavior visible only for sizes bigger than 80^3 spins while the STA or bct helimagnets show a second-order transition for similar sizes.

Furthermore the size of this region of low velocity will vary as a function of the distance between the complex fixed point F_+ and the real plane shown in Fig. 10a. It has been shown that N_c, where the two fixed points F_- and F_+ collapse and become complex, is bigger than 3 and the distance of F_+ to the real plane will be larger for $N = 2$ than for $N = 3$. Therefore the size of the domain of low velocity will be bigger for $N = 3$ than for $N = 2$, and the true first-order behavior will be seen for smaller sizes in the XY case ($N = 2$) than in the Heisenberg case ($N = 3$). Indeed the first-order transition in the dihedral, STAR and STA can be seen from the size 12, 18 and 96, respectively, for XY spin systems (see Table 4). For Heisenberg spins this has been seen for the dihedral model with a size $L = 80$ (see Table 6) while the estimate size for the STA should be larger than 800.[8] We note that a first-order transition has been found in quasi–one–dimensional STA[9]: the initial point in the flow diagram is outside the domain of low velocity.

For the XY case Delamotte et al.[48] using a non perturbative RG approach, found that there is no minimum in the flow but always a low velocity region (outer circle of Fig. 10b). Following the initial point in the RG flow the systems will show different sets of exponents, i.e. the system is in a crossover region. Numerical simulations tend to support this interpretation. Indeed for XY spins the STAR and the STA for small sizes ($L < 40$) display a second-order transition with different critical exponents (see Tables 4-5) and for large sizes the STA shows a first-order transition as discussed above.[8]

In conclusion the transition for Heisenberg spins is of first order but an "almost second-order transition" could exist for a range of "finite" sizes. This "almost second-order transition" will have a set of exponents different from the ferromagnetic ones because the breakdown of symmetry is different: $O(N)/O(N-2)$ in comparison to $O(N)/O(N-1)$ for ferromagnetic systems. This "new" universality class has been called chiral class.[5] For the XY case there is a crossover region with a slow velocity and exponents will vary between those of the chiral class and of weak first-order transitions ($\nu = 1/3$ ...- see Table 1). The critical exponents of this chiral class are given in Tables 4-8 for N varying from 2 to 6 for the STA, STAR, and dihedral models. With numerical simulations, exponents γ/ν β/ν and ν are usually calculated using finite size scaling while other exponents are calculated using the scaling relation $d\nu = 2 - \alpha$ and $\gamma/\nu = 2 - \eta$ (see 6).

There is another indication given by Loison and Schotte[34] which suggests that the phase transition is indeed due of a "complex fixed point'. Using the scaling formula $\gamma/\nu = 2 - \eta$, one gets a negative η for $N = 2$ and $N = 3$ for the STA, STAR or dihedral model (see Tables 4-8) which contradicts the theorem that η must be always positive.[46,47] Negative η can also be calculated using experimental results.[48] Therefore the fixed point cannot be real. Using this indication we can conclude that the continuous transition found in fully frustrated XY lattice[23] is indeed of first order.

Table 4. Critical exponents associated to the $SO(2)$ symmetry by Monte Carlo for XY spins ($N = 2$) and a BS $Z_2 \otimes SO(2)$. $^{(a)}$Calculated by $\gamma/\nu = 2-\eta$. The first result[5] comes from a study at high and low temperatures and uses the FSS. The second[6] uses the Binder parameter to find T_c and uses the FSS, the third[7] uses the maxima in FSS region.

system	Ref.	L_{max}	α	β	γ	ν	η
STA	[5]	60	0.34(6)	0.253(10)	1.13(5)	0.54(2)	-0.09(8)$^{(a)}$
STA	[6]	33	0.46(10)	0.24(2)	1.03(4)	0.50(1)	-0.06(4)$^{(a)}$
STA	[7]	36	0.43(10)			0.48(2)	
STA	[8]	126	first order				
STA	[9]	35	first order				
bct	[19]	24	first order				
STAR	[34]	36	first order				
$V_{2,2}$	[34]	36	first order				

Table 5. Critical exponents associated to the Z_2 symmetry (chirality κ) by Monte Carlo for XY spins ($N = 2$) and a BS $Z_2 \otimes SO(2)$. $^{(a)}$Calculated by $\gamma/\nu = 2 - \eta$. The first result [5] comes from a study at high and low temperature and uses of FSS. The second [6] uses the Binder parameter to find T_c and uses the FSS.

system	Ref.	L_{max}	α	β_κ	γ_κ	ν_κ	η_κ
STA	[5]	60	0.34(6)	0.55(4)	0.72(8)	0.60(3)	0.80(19)$^{(a)}$
STA	[6]	33	0.46(10)	0.38(1)	0.90(2)	0.55(1)	0.28(3)$^{(a)}$
STA	[8]	126	first order				
STA	[9]	35	first order				
bct	[19]	24	first order				
STAR	[34]	36	first order				
$V_{2,2}$	[34]	36	first order				

Table 6. Critical exponents by Monte Carlo for Heisenberg spins ($N = 3$) and a BS $SO(3)$. Calculated by $^{(a)}$ $\gamma/\nu = 2 - \eta$, $^{(b)}$ $d\nu = 2 - \alpha$, $^{(c)}$ $2\beta/\nu = d - 2 + \eta$.

system	Ref.	L_{max}	α	β	γ	ν	η
STA	[5]	60	0.240(80)	0.300(20)	1.170(70)	0.590(20)	+0.020(180)$^{(a)}$
STA	[10]	36	0.242(24)$^{(b)}$	0.285(11)	1.185(3)	0.586(8)	-0.033(19)$^{(a)}$
STA	[12]	48	0.245(27)$^{(b)}$	0.289(15)	1.176(26)	0.585(9)	-0.011(14)$^{(a)}$
STA	[11]	36	0.230(30)$^{(b)}$	0.280(15)		0.590(10)	0.000(40)$^{(c)}$
bct	[20]	42	0.287(30)$^{(b)}$	0.247(10)	1.217(32)	0.571(10)	-0.131(18)$^{(a)}$
STAR	[35]	42	0.488(30)$^{(b)}$	0.221(9)	1.074(29)	0.504(10)	-0.131(13)$^{(a)}$
$V_{3,2}$	[35]	40	0.479(24)$^{(b)}$	0.193(4)	1.136(23)	0.507(8)	-0.240(10)$^{(a)}$
$V_{3,2}$	[8]	80	first order				

Table 7. Critical exponents by Monte Carlo for spins with four components ($N = 4$) and a BS $O(4)/O(2) \equiv SO(4)/SO(2)$. Calculated by $^{(a)}$ $\gamma/\nu = 2 - \eta$, $^{(b)}$ $d\nu = 2 - \alpha$.

system	Ref.	L_{max}	α	β	γ	ν	η
STAR	[36]	42	0.287(27)$^{(b)}$	0.291(11)	1.133(28)	0.571(9)	+0.015(18)$^{(a)}$
$V_{4,2}$	[36]	40	0.278(30)$^{(b)}$	0.290(12)	1.142(34)	0.574(10)	+0.011(25)$^{(a)}$

3.1.4. *Experiment*

A resembling situation occurs in the analysis of experiments. There the correlation length ξ plays the role of the system size in numerical simu-

Table 8. Critical exponents by Monte Carlo for spins with six components ($N = 6$) and a BS $O(6)/O(4) \equiv SO(6)/SO(4)$. Calculated by $^{(a)}$ $\gamma/\nu = 2 - \eta$, $^{(b)}$ $d\nu = 2 - \alpha$.

system	Ref.	L_{max}	α	β	γ	ν	η
STA	[13]	36	-0.100(33)$^{(b)}$	0.359(14)	1.383(36)	0.700(11)	+0.025(20)$^{(a)}$

lations. For a second-order transition one has $\xi \sim (T - T_c)^{-\nu}$. Therefore we should observe a crossover between the region of low velocity ("almost second-order transition" in Zumbach's words) to the true first-order behavior for temperatures "closer" to the critical temperature. Unfortunately the situation is even more complicated in experimental systems with the omnipresence of planar or axial anisotropies and the one- or two-dimensional characters of the compounds. Then a succession of crossovers (see 6 for more details about crossovers) from 2d to 3d and from Heisenberg to Ising or XY behavior could lead to difficulties in the interpretation. Furthermore other (small) interactions could also dominate the behavior near the critical temperature and change the universality class.

Experiments for XY spins: All experimental results can be found in Ref. [34]. Several AXB_3 compounds have the STA structure. The experiments on $CsMnBr_3$,[49,50,51,52,53,54,55,56,57,58,59] $RbMnBr_3$[60,61] and $CsVBr_3$[62] give critical exponents compatible with those of MC simulation on STA and a second-order transition. We can interpret this result by the fact that the systems are under the influence of a complex fixed point, and $t \propto T - T_c$ is too small to observe a first-order transition.

The case $CsCuCl_3$[63] is different since the authors observe a crossover from a second-order region with exponents compatible with MC results on STA for $10^{-3} < t < 5.10^{-2}$ to a region of first-order transition for $5.10^{-5} < t < 5.10^{-3}$. For $t < t_0 \approx 10^{-3}$ one seems to observe the true first-order region which corroborates the scenario introduced previously.

Three kinds of helimagnetic structure have been studied: Holmium, Dysprosium and Terbium. Essentially three types of results exist: those compatible with MC ones of the STA, those with a large β incompatible with STA and those showing a weak first-order transition.

The results compatible with those of MC on STA for Ho [65,67,66] Dy[66,73,74] and Tb[78,79,80,81,82] can be interpreted as before: the systems are under the influence of F_+. The first-order transition for Ho[64] and Dy[71,72] is due to the fact that the measurements were done in the first-order region near the transition temperature. The values of the exponent $\beta \sim 0.39$ in the

case of Ho[67,68,69,70] and Dy[68,75,76,77] are not compatible with those found by MC ($\beta \sim 0.25$). This fact can be explained by the presence of a second length scale in the critical fluctuations near T_c related to random strain fields which are localized at or near the sample surface.[67] Thus the critical exponent β measured depends on this second length.

Experiments for Heisenberg spins: All experimental results can be found in Ref. [34]. As explained previously, before the first-order region is reached, the crossover from Heisenberg to Ising or XY behavior prevents a first-order transition of Heisenberg type. Nevertheless the second-order transition can be studied for VCl_2,[83] VBr_2[84], $Cu(HCOO)_2 2CO(ND_2)_2 2D_2O$[85] and $Fe[S_2CN(C_2H_5)_2]_2Cl$.[86] For the last two examples the observed exponents might be influenced by the crossover from 2d to 3d Ising behavior. The experimental results agree quite well with the MC simulations.

3.1.5. *Value of N_c*

Tables 4-8 allow us to get an idea of the value of N_c. The MCRG gives an estimate $3 < N_c < 8$ but the values of η can give a better estimate following Ref. [34]. As can be seen for the XY and Heisenberg systems, negative values of η appear for the STA, STAR or dihedral model. But η must always be positive.[46,47] This is due to the use of the scaling relation $\gamma/\nu = 2 - \eta$. Indeed Zumbach[45] has shown that for an "almost second-order transition", i.e. when the solution becomes complex, this relation has to be modified to $\gamma/\nu = 2 - \eta + c$, c being a constant different from zero. We can use this relation as a criterion for real or complex fixed points. In three dimensions η is usually small and is almost independent of N for the ferromagnetic case, that is ~ 0.03 (see Table 1). Our hypothesis is that it is also true for the frustrated case. Indeed for $N = 6$ we found $\eta \sim 0.03$ (see Table 8). Accepting this value c becomes zero around $N_c \sim 4.5$. Obviously if a bigger value of η is chosen, N_c will increase.

3.1.6. *Phase diagram (N,d)*

In Fig. 11 we have plotted a phase diagram where the abscissa is the spin dimension N and the ordinate the space dimension d.

There is a line which divides a region of first-order transition from a region of second-order transition. At, and near, $d = 4$ we can use the RG $d = 4 - \epsilon$ expansion to find $N_c = 21.8 - 23.4\,\epsilon$, and for $d = 3$ we have seen that

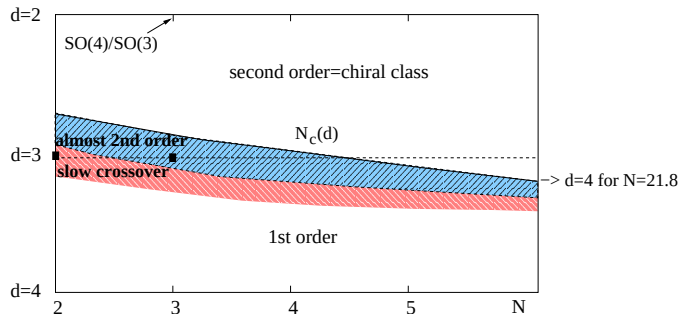

Fig. 11. The critical curve $N_c(d)$ separating the first-order region for small N and large d from the second-order region for large N and low d. The squares represent the physical systems of interest ($N = 2, 3$ in three dimensions).

$N_c \sim 4.5$. Furthermore there is a region near this line where the transition is "almost second order", i.e. under the influence of the complex fixed point for "small" sizes. The system will display a second-order transition with stable critical exponents. Besides, there is a slow crossover region where critical exponents vary with the system size. The sizes of these regions depend on the initial point in the flow diagram and therefore on the model.

Near two dimensions and for Heisenberg spins the transition is of the type $SO(4)/SO(3)$, i.e. ferromagnetic for spins with four components (see the following section and the chapter of Delamotte et al.[32] for more details).

3.1.7. *Renormalization-Group expansions*

We present here a review of the RG expansions ("non perturbative", $d = 4 - \epsilon$, in fixed dimension $d = 3$, and $d = 2 + \epsilon$). For more details see 6 and the chapter of this book of Delamotte et al.[32]

We discuss now the $4-\epsilon$ expansion. Using a continuous limit of the Landau Ginzburg Hamiltonian (6), it involves a perturbative extension (u, v) around the Gaussian solution with the dimension d and the number of spin components N as parameters. To get the result for $d = 3$ one puts $\epsilon = 1$. Of course the series are at best asymptotic and must be resummed, even for the ferromagnetic case .[87] The extension until ϵ^2 in Ref. [88] has been "resummed" (only three terms) and the value of $N_c(d = 3) \sim 3.39$ is compatible with the numerical result $N_c^{numerical}(d = 3) \sim 4.5$. The calculations have been extended to ϵ^4 in Ref. [89] but unfortunately no resummation has been done on this series yet.

The expansion for fixed dimension $d = 3$ is very similar to the $d = 4 - \epsilon$ one. The series and the resummation will differ slightly. At three loops the result is $N_c \sim 3.91$[90] which is again not far from $N_c^{numerical}(d = 3) \sim 4.5$. A very interesting picture emerges from the six-loop calculations.[91,92] First, for $N \sim 5$, the resummation does not converge. Second, for $N = 3$, the resummation gives rise to a very large variation of the critical exponents following the flow chosen to arrive at a single critical exponent at the critical point (see Fig. 5 of the reference[92]) which is a really "new" phenomenon. Third, for $N = 2$ a second-order transition is predicted in contradiction to Itakura's results[8] and the numerical simulations (see Tables 4-5). Manifestly we could conclude that the resummation chosen does not work for this series. To understand this we have to stress that the series has many more terms because of the double expansions in u and v compared to a single one for the ferromagnetic case. Whence it is much more difficult to find a "good" resummation scheme.

On the other hand Delamotte et al.[93] found that the transition must be of $SO(4)/SO(3)$ type, i.e. equivalent to a ferromagnetic $O(4)$ transition, near two dimension for Heisenberg spins. This study was done using the $d = 2 + \epsilon$ expansion or equivalently the non linear σ model and the result is valid only near two dimensions. This prediction was checked by Southern and Young[94] by MC in two dimensions. But we can give arguments[35] using $1/N$–expansion and the value of the critical exponents to rule out this kind of transition in three dimensions. These arguments hold as long as the relevant operators are identical in $1/N$ expansion and in the non linear σ model. Indeed for the $1/N$ expansion, and equivalently for the $4 - \epsilon$ expansion and in fixed dimension, we keep in the Hamiltonian only the terms which are renormalizable near $d = 4$ or infinite N, and discard the others. Nevertheless it seems that some non renormalizable terms (see 6) become relevant and important for low N and d and, whatever the number of loops we cannot find the correct behavior using these expansions.

Because of the problems encountered by the standard expansions, a "non perturbative" approach could be very useful. This was introduced in this model by Tissier et al.[48] We quote "non perturbative" because it is not an expansion resembling the other methods where the extension parameters (u, v, ϵ) are usually not small. In this non perturbative method even if we introduce only a few terms in the action, results will be very good and no resummation is necessary. We notice that the simplest action was studied by Zumbach[45] which allows him to introduce the "almost second-order" transition. Adding more terms, Tissier at al. found that they are able to

retrieve all the previous expansions with additional information. Their value of $N_c \sim 5.1$ is comparable to $N_c^{numerical} \sim 4.5$. In three dimensions they found critical exponents very close to those calculated by MC for $N = 6$ (see Table 8), a minimum in the flow for $N = 3$, and a slow crossover for $N = 2$ as explained in the previous section. They found also that the critical behavior is indeed that of a ferromagnetic $O(4)$ transition near two dimensions for Heisenberg spins. Some non–renormalizable operators excluded in the $4-\epsilon$ and $1/N$ expansions are included in this "non perturbative" method. These operators are always relevant between two and four dimensions whatever N is, but have an influence on the values of the critical exponents only for small N and near two dimensions. This explains the discrepancy between the $d = 2 + \epsilon$ and $d = 4 - \epsilon$ expansions.

3.1.8. *Short historical review*

In this section we give a short historical review of studies on frustrated systems. Indeed the history was not straight if we look back at the last 25 years. The development began by a RG $4 - \epsilon$ expansion by Jones, Love and Moore[95] in 1978. It is only in 1984 and in the following years that Kawamura[5] started with the first numerical simulations and, in combination with the results of several experiments, proposed a "new" universality class.

Then Azaria, Delamotte et al[93] found that the transition near two dimensions for Heisenberg spins should belong to the $O(4)$ ferromagnetic class. Several groups (see Tables 4-8) have done numerical simulations and experiments which favored either the new universality class, a first-order transition, an $O(4)$ transition and even a mean-field tricritical transition. During those years Sokolov et al.[88,90] have extended the RG expansion to three loops and found a first-order behavior for XY and Heisenberg spins.

Surely one of the most important articles to find the key to understand the physics was written by Zumbach,[45] using a non perturbative approach. He predicts an "almost second-order transition" for XY and Heisenberg spins. Loison and Schotte,[34,35] using this concept, were able to get a clear picture for both the numerical and experimental studies. Then Tissier, Delamotte and Mouhanna,[48], by extending the work of Zumbach, were able to understand the whole phase diagram for the dimension between two and four. To terminate Itakura,[8] confirmed the picture given by Zumbach&Loison&Schotte, which we think is the definitive answer from a numerical point of view.

3.1.9. *Relations with the Potts model*

We would like now to stress the similarities between the Potts model and the frustrated case just studied.[44] In Fig. 12 we have plotted the RG flow diagram[96] as a function of the first- and second-neighbor ferromagnetic interactions (J_1 and J_2) and the chemical potential Δ (corresponding to the site vacancy).

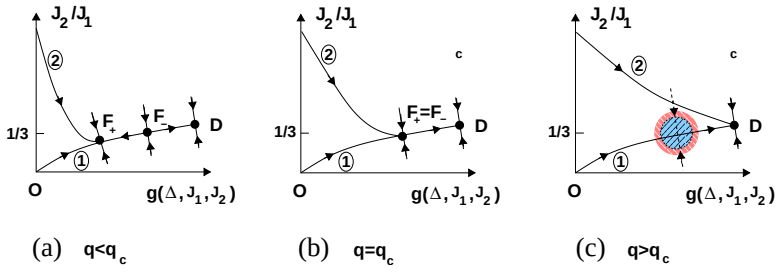

Fig. 12. Hypothesis of the renormalization flow in presence of second-neighbor interaction. For $q \leq q_c$ the initial point of the flow is irrelevant to the critical behavior. For $q > q_c$ the behavior for accessible lattice size will be different for the curve 1 (going through the basin of attraction of the fixed points F_+) and the curve 2 (going directly to the first-order fixed point D).

F_+ is the standard stable ferromagnetic fixed point and F_- is an unstable fixed point. D is a first-order fixed point. O is the initial point of the system. This figure resembles the one of the frustrated case (Fig. 9). For $q < q_c$ the flow goes to the fixed point F_+ and has a second-order transition. At $q = q_c = 4$ (in two dimensions) the two points F_+ and F_- collapse and a second-order phase transition with logarithm correction results. For $q > q_c$ there is no longer a solution and the flow goes directly to the fixed point D, i.e. the system has a first-order transition. Our hypothesis is that even if the solution of F_+ is complex, it has an influence on the real space and there is a region of low velocity in the flow diagram. It can be a true minimum for $q \gtrsim q_c$ with an "almost" second-order transition. For q bigger, no minimum should exist but, following the sizes studied, a variation of the critical exponents could occur. Indeed for $q = 5$ a set of critical exponents was found,[43] corresponding to our hypothesis of "almost second-order" transition. The cases $q = 6$ and $q = 7$ have not been studied, but possibly one could observe a variation of critical exponents corresponding to a slow crossover to the first-order point.

We remark that depending of q we can observe clearly if the transition is of first order or second order. In Fig. 12 we have plotted the flow (2) in presence of the second-neighbor interaction. We observe that this flow is less influenced by the low velocity region than the flow (1) if $q > q_c$ and it reaches F_+ if $q \leq q_c$. Adding the third-nearest-neighbor interaction, we are able to find numerically that $q_c = 4$ for the crossover from the first-order to second-order transitions. Contrary to the frustrated case we know roughly the coordinate of the fixed point F_+ ($J_2/J_1 \sim 0.3$)[97] and $\Delta \neq 0$.[96] By consequence we know which kind of interaction must be added.

3.2. $O(N)/O(N-P)$ breakdown of symmetry for $d = 3$

In mean-field theory, for $N > P$ the model shows a usual second-order type, but for $N = P$ the transition is a special one.[45] The BS in this case is $Z_2 \otimes SO(N)$ and the coupling between the two symmetries leads to a special behavior which, for $N = P = 2$ in two dimensions, has been extensively debated (see later in this chapter).

These generalized chiral models have been studied by applying the RG technique ($d = 4 - \epsilon$ expansion).[45,98,99] The picture is very similar for all $N \geq P \geq 2$. At the lowest order in ϵ, there are up to four fixed points, depending on the values of N and P. Amongst them are the trivial Gaussian fixed point and the standard isotropic $O(NP)$ Heisenberg fixed point. These two fixed points are unstable. In addition, a pair of new fixed points, one stable and the other unstable, appear when $N \geq N_c(d)$ with

$$N_c(d) = 5P + 2 + 2\sqrt{6(P+2)(P-1)} - \left[5P + 2 + \frac{25P^2 + 22P - 32}{2\sqrt{6(P+2)(P-1)}}\right]\epsilon\,. \tag{8}$$

For $P = 2$ we find the standard result $N_c = 21.8 - 23.4\,\epsilon$. On the other hand, for $P = 3$ we obtain $N_c = 32.5 - 33.7\,\epsilon$ and for $P = 4$ we obtain $N_c = 42.8 - 43.9\,\epsilon$. A "tricritical" line exists which separates a second-order region for low d and large N from a first-order region for large d and small N. Applying $\epsilon = 1$ ($d = 3$), we obtained that $N_c(d = 3) < 0$ for all P. For $P = 2$ we know that this result does not hold and equivalently it does not apply for $P \geq 3$. Loison[39] has done some simulations for $N = 3$ and $N = 4$ with $P = N$ and $P = N - 1$ for the Stiefel $V_{N,P}$ model. He showed that the transition is clearly of first order using numerical simulations. He generalized this result for all N. We remark that the fully frustrated cubic lattice (generalized Villain lattice) which could have an identical BS has also

a first-order transition for Heisenberg spins.[25] In conclusion the transition in systems with a $O(N)/O(N-P)$ the breakdown of symmetry is of first order for $P = N$ and $P = N-1$ and in particular for the physical case $N = P = 3$, i.e. a non planar GS for Heisenberg spins.

3.3. $Z_2 \otimes SO(N)/SO(N-1)$ breakdown of symmetry for $d = 3$

For $N > 2$, this BS corresponds to a collinear ground state associated to a BS of the lattice (see Table 2-3). For example the stacked Villain lattices with first-neighbor ferromagnetic interaction J_1 and a second-neighbor antiferromagnetic interaction J_2 can have this BS. For $J_2/J_1 < -0.5$ the competition between the two interactions leads to two possible ground states.[22] For $N = 2$ (XY spins) the stacked Villain lattices and the stacked J_1–J_2 model have the same BS as the STA and should display an analogous behavior ("almost second order" for small sizes following by a first-order transition for larger sizes).

We have simulated by MC technique the stacked Villain lattices and the stacked J_1–J_2 lattice which have this kind of BS. We found that the transition seems continuous[40] for small lattices for XY and Heisenberg spins. For XY spins this is in agreement with the numerical simulation of STA which has an identical BS. We have also studied the Ising–$V_{N,1}$ model which has the same BS. For $N = 2$ this model is the equivalent to the $V_{2,2}$ model which has a strong first-order behavior as explained previously. For $N = 3$ and $N = 4$ we found also strong first-order transitions. Therefore it seems that the transition $Z_2 \otimes SO(N)/SO(N-1)$ is of first order for any N even if it could exist an "almost second-order transition" for small sizes.

3.4. $Z_3 \otimes SO(N)/SO(N-1)$ breakdown of symmetry for $d = 3$

This BS appears with a collinear ground state associated to a three-state Potts symmetry due to breakdown of lattice symmetries. This corresponds to various lattices where the unit cell is composed of four spins (two parallel spins and two antiparallel spins) like the STA with intermediate NNN interaction ($0.125 < J_2/J_1 < 1$), the fcc, the hcp, the cubic J_1–J_2 model or the pyrochlore (see Table 2-3).

As seen previously, even the coupling of an Ising symmetry (Z_2) with $SO(N)/SO(N-1)$ can give a first-order transition. Whence it is expected that the transition with a three-state Potts symmetry (Z_3) gives also a

first-order transition which is even stronger if we consider that the Potts symmetry alone has a first-order transition in $d = 3$ for $q = 3$. Indeed a strong first-order transition was seen in the fcc,[25,28] hcp,[29] cubic J_1–J_2 model[25,26] pyrochlore[30] and STA with NNN interaction[7,11] for XY and Heisenberg spins.

We have done some simulations for the Potts–$V_{N,1}$ model with the Hamiltonian (5) with $q \geq 3$, i.e. the q-state Potts model coupled to an N-component vector. We found a strong first-order transition for any N and q.

In conclusion the transition for the $Z_q \otimes SO(N)/SO(N-1)$ BS in $d = 3$ is of first order for any $N \geq 2$ and $q \geq 2$.

3.5. $Z_q \otimes O(N)/O(N-2)$ and other breakdown of symmetry in $d = 3$

This BS appears with a planar ground state associated to a three-state Potts symmetry. One example is the STA with NNN interaction $J_2/J_1 > 1$ (see Table 2-3).

To simulate this BS we have used a Potts–$V_{N,2}$ model for any q. We found the behavior of a strong first-order transition whatever N and q are. It is not surprising if we consider that the "less frustrated" model Potts–$V_{N,1}$ is already of first order.

We have also simulated the $Z_q \otimes O(N)/O(N-3)$ for $N = 3$ which corresponds to the BS $Z_q \otimes Z_2 \otimes SO(N)$ using a Potts–$V_{N,P}$ model. We found again a strong first-order transition. Similar results are obtained for Ising–Potts–$V_{N,1}$ and Ising–Potts–$V_{N,2}$ models.

To summarize, it seems that the coupling between a Potts or Ising symmetry and a continuous symmetry of vector spins give always rise to a first-order transition.

4. Conclusion

We have studied breakdowns of symmetry of three-dimensional lattices for XY ($N = 2$) and Heisenberg ($N = 3$) spins. The general form of the breakdown of symmetry is $S_{lattice} \otimes O(N)/O(N-P)$. $S_{lattice}$ is usually a Potts symmetry Z_q (Z_1 corresponds to the identity, Z_2 to an Ising symmetry, Z_3 to a three-state Potts symmetry, ...). P runs from 1 to 3.

If the frustration is small the GS can be collinear ($P = 1$) without breaking any symmetry of the lattice $S_{lattice} = 1$, the BS will be $SO(N)/SO(N-1)$ and the transition will be of second order like in ferro-

magnetic systems.

If the frustration is strong enough, we can have a non collinear GS with the usual planar configuration ($P = 2$) like in the STA or helimagnets and $S_{lattice} = 1$. Depending on the model and for not "too big" sizes, the transition could appear continuous belonging to a new universality class. For an infinite size the system will have a first-order transition.

Some more complicated systems could also have a non planar GS, and for Heisenberg spins it corresponds to $P = 3$ with usually $S_{lattice} = 1$. The transition will be of first order with a possible "almost second-order" behavior for small system sizes similar to the $P = 2$ case.

Some even more complicated systems could have a non collinear GS ($P = 2$ or $P = 3$) with $S_{lattice} = Z_q$ and $q = 3$. For example the STA with large NNN interaction has a strong first-order transition.

On the other hand some frustrated systems have degenerate GS but by "order by disorder" a collinear GS ($P = 1$) is selected. The lattice symmetry could be broken giving an additional BS. $S_{lattice} = Z_2$ (Ising) for the stacked Villain model, or $S_{lattice} = Z_3$ in fcc, hcp, STA with intermediate NNN interaction, and pyrochlore. For the Z_3 symmetry the transition is strongly of first order even for small sizes. For the Z_2 symmetry the transition is also of first order for large sizes but looks continuous for small sizes. Therefore we cannot exclude an "almost second-order" behavior belonging to a new universality class.

In conclusion frustrated systems have a first-order transition for XY and Heisenberg spins in three dimensions even if for "small" sizes the systems would show a second-order transition. "Small" could mean sizes of thousands of lattice constants and the first-order transition will then not be observable with the actual computer resources.

5. $O(N)$ frustrated vector spins in $d = 2$

5.1. *Introduction*

The situations in two-dimensional systems are different from the three dimensions. The Mermin–Wagner theorem[100] asserts that no magnetization appears at non-zero temperature. However, a transition due to the topological defects[101,102] can appear. The binding–unbinding transition of vortex–antivortex pairs for XY spin systems is a classical example. We note that their exact role for three-dimensional phase transitions is not clear.[103,104,105] For non collinear GS, the topological properties of the system differ from those of collinear GS and new types of transition could

appear. In the following we will briefly review the ferromagnetic case, then the frustrated XY case, applicable to Josephson–junction arrays in magnetic fields, and finally the frustrated Heisenberg cases.

5.2. *Non frustrated XY spin systems*

For a non frustrated XY spin system the order parameter is $SO(2)$. The topological defects of this group is only the point defect classified by the homotopy group $\Pi_1(SO(2)) = Z$, Z being the topological quantum number of the defect.[101,102] A Kosterlitz–Thouless (KT) transition [106] exists at the critical temperature $T_c \sim 0.9$, driven by the unbounding of vortex–antivortex pairs.

This transition has some special features: for $T < T_c$ the correlation length (ξ) is infinite, while for $T > T_c$ it has an exponential decreasing contrary to the power-law behavior in the standard transition.

Several numerical methods exist to calculate the critical temperature and the critical exponents (see 6).

5.3. *Frustrated XY spin systems: $Z_2 \otimes SO(2)$*

A frustrated XY spin system can have many order parameters as previously seen (see Table 2). The most studied case is $Z_2 \otimes SO(2)$ which corresponds to a non collinear GS: triangular lattice,[107,108,109,110,111] Villain lattice or two-dimensional fully frustrated lattice[107,4,112,113,114,115,116,117,118,119] and related Zig–Zag models.[31,120] In combination to the topological defect point Z, there is a line of Z_2 corresponding to an Ising transition. Therefore they will have similar properties as the J_1–J_2 model, the $V_{2,2}$ model or any model where the Z_2 symmetry comes from the lattice. We note that different models can have an identical group and therefore the same topological defects. The following models should have analogous properties: the Villain model on the Villain lattice,[123] The Ising–$V_{2,1} \equiv V_{2,2}$ model,[121,122] the 19-vertex model,[124] the $1D$ quantum spins,[125] the Coulomb gas representation,[126,127,128,129] the $XY - XY$ model,[130,131] or the RSOS model.[132]

This kind of models was widely studied because it is believed to correspond to experimental systems such as Josephson–Junction arrays of weakly coupled superconducting islands[133,134] or films of Helium ^{3}He.[135,136,137,138]

The question is to understand the coupling between the vortex–antivortex and the Ising symmetry. Contrary to the three-dimensional case discussed previously there are no clear accepted answers to these questions.

We will therefore only present the different results in the high temperature region and in the FSS, giving some clues to understand the physics of theses systems.

What are the possible scenarios?

1. $T_c^{KT} < T_c^{Ising}$
   The KT transition associated to the topological defects appears at a temperature lower than the one associated to the Ising transition even if they can be very close. The two transitions should have standard behaviors ($\nu^{KT} = 0.5$, $\nu^{Ising} = 1, \cdots$).
   Furthermore Olsson has proposed that the Ising behavior could be observed only when $L \gg \xi^{KT}$. Since ξ^{KT} is infinite for $T \leq T_c^{KT}$ and decreases exponentially for $T > T_c$, it will correspond to a high temperature region with $T \gg T_c^{KT}$, but also $T \gg T_c^{Ising}$ when the two transitions appear in close neighborhood. In particular the FSS region will have a non standard Ising behavior for the sizes accessible with actual computer resources. Only for a very large lattice the standard Ising behavior will be visible. We observe the similarity of this hypothesis with the one described previously in three dimensions and we could call the transition in the FSS an "almost new Ising–KT behavior".
2. $T_c^{KT} \sim T_c^{Ising}$
   The two transitions appear at the same temperature and display different behaviors compared to the standard one. We remark that for high temperatures $T \gg T_c$, i.e. in the high-temperature region, we cannot assume that the coupling between the Z_2 symmetry and the topological defects would be identical as for $T \sim T_c$. Indeed with a lot of small Z_2 walls dividing the system it is not certain that the vortex and the antivortex should play an important role and we could get a standard Ising transition.
3. $T_c^{KT} > T_c^{Ising}$
   This hypothesis was advanced by Garel et Doniach in 1980 for the J_1–J_2 model,[139] but numerical MC simulations have shown that it is not the case[22] for this system.

To choose the most probable hypothesis we will look now at the numerical results:

Some information can be provided by numerical MC simulations in the high-temperature region. Fitting the results it is possible to get the critical temperature and the critical exponents. Because of the presence of correc-

tions and by consequence of many free parameters, the extraction of the results is difficult.

For the Ising symmetry Olsson[123] has found a standard ferromagnetic one with $\nu^{Ising} \sim 1$) while Jose and Ramirez[115] found $\nu^{Ising} \sim 0.87$. New simulations should be done to resolve this discrepancy. If $\nu^{Ising} \neq 1$, it will a counter–proof to Olsson's claim (first possibility). On the other hand, if $\nu^{Ising} = 1$, we cannot rule out the second possibility.

The exponent of the KT transition have been only calculated by Jose and Ramirez.[115] They found non standard $\nu^{KT} \sim 0.3$ to be compared to 0.5 in the ferromagnetic case. If this result is in favor of the second hypothesis, it cannot rule out the first one. Indeed we can reverse the argument given at the end of the second hypothesis. If at high temperatures the system is composed of many domains separated by walls of Z_2, the correlation between the topological defects could not be the one of the standard one. Therefore there is no definitive conclusion from the high-temperature simulations.

Now we can look at the results in the FSS.
For the Ising transition the critical exponents have been precisely determined by Loison and Simon,[22,111] for the J_1–J_2 model using both the FSS and the dynamical properties including the first correction[111] due to the lattice size L. They obtained non standard critical exponents $\nu^{Ising} = 0.815(20)$. The "large" error is due to the inclusion of the corrections. See Ref. [111] for a review of all the numerical works. For the triangular lattice the critical temperature is known with high precision $T_c^{Ising} = 0.5122(1)$.
The KT transition is more problematic. First we can use the helicity[106] Υ to find the critical temperature. If we admit the same universal jump at the critical temperature as the ferromagnetic one, we get $T_c^{KT} = 0.5010(10)$ a temperature much smaller than $T_c^{Ising} = 0.5122(1)$. But we cannot be sure that $\Upsilon_{jump}^{frustrated} = \Upsilon_{jump}^{ferromagnetic}$ and this result must be taken with care.
As explained in the previous section we can use the Binder parameter or the dynamical properties of the model to calculate T_c^{KT} and the critical exponents. Using this method we found very interesting results. First the Binder parameter shows a power-law transition and not an exponential one. In addition the critical exponents and temperatures calculated by the two methods are in good agreement with $T_c^{KT} = 0.5102(2)$ just below $T_c^{Ising} = 0.5122(1)$ for the triangular lattice. The critical exponent $\eta^{KT} = 0.36(1)$ is very different from the standard one 0.25. These results are in accord with those on the J_1–J_2 model. What is disturbing is that for the triangular lattice, accepting $T_c^{KT} = 0.5102(2)$, the helicity jump is

smaller than the $\Upsilon_{jump}^{ferromagnetic}$ although it is believed that it should be greater.
The situation is puzzling with no definitive conclusions.

5.4. *Frustrated XY spin systems: $Z_3 \otimes SO(2)$*

Two-dimensional systems with an order parameter like $Z_3 \otimes SO(2)$ are less numerous than three-dimensional systems. Following Table 2 we know at least two systems: the triangular lattice with intermediate NNN interaction and the Potts–$V_{2,1}$ model.

No numerical studies have been done for the former system, but we have studied[141] the latter one. It gives a first-order transition.

Following the reasoning of the previous section two principal hypotheses appear:

1. Olsson hypothesis: KT transition at lower temperature following the transition associated to the Potts symmetry Z_3 at higher temperature. Non standard critical exponents should appear in the FSS region due to a screening length (ξ^{KT}). The "true" standard second-order behavior will appear only for very large lattices ($L \gg \xi^{KT}$) or in the high-temperature region.
2. A new behavior for the KT and Potts transitions at the same critical temperature.

The results are in favor of the second hypothesis. The Potts symmetry has a first-order transition. It means that its correlation length ξ_{Z_3} is finite at the critical temperature and less than ξ_{KT}. There will be no change even if the system size L is much larger and the system will never show a standard three-state Potts second-order transition. Obviously we cannot apply directly this result to the Ising–KT transition since the two models are not equivalent although it is nevertheless an argument against the Olsson's hypothesis.

5.5. *Frustrated XY spin systems: $Z_2 \otimes Z_2 \otimes SO(2)$ and $Z_3 \otimes Z_2 \otimes SO(2)$*

Following Table 2 the order parameter $Z_2 \otimes Z_2 \otimes SO(2)$ can appear with a J_1–J_2–J_3 lattice or an Ising-$V_{2,2}$ model. In addition $Z_3 \otimes Z_2 \otimes SO(2)$ exists in the triangular antiferromagnetic with NNN interaction and in the Potts–$V_{2,2}$ model. No numerical studies have been done on these models.

5.6. *Frustrated Heisenberg spin systems: SO(3)*

For a non frustrated Heisenberg spin system the order parameter will be $SO(3)/SO(2)$ and no topological defects exist in two dimensions, no phase transition will appear.

For a frustrated system many order parameters can exist (see Table 3), but only the planar GS have received attention. In this case the order parameter is $SO(3)$ and there exist point defects that is Z_2–vortex–antivortex[101,102]. These topological defects are different from the Z–vortex present in XY systems. The existence of a critical transition driven by the unbounding of vortex–antivortex was first conjectured by Kawamura and Miyashita.[142]

At low temperatures the spin waves will dominate the behavior of the system and forbid an infinite correlation length below T_c contrary to XY spins. The behavior should be equivalent to the one present in the four-dimensional ferromagnetic system.[93] This conjecture based on the non linear σ model ($d = 2+\epsilon$ expansion) and on symmetry arguments was checked by Southern and Young[94] and Caffarel et al.[143]

At higher temperatures the topological defects will clearly have a role.[143,144,145,146]
Caffarel et al.[143] have studied numerically two models having identical spin waves but not the same topological defects. One has the topological Z_2 defects, the other not. They showed that the two models are equivalent at low temperatures, but show differences at higher temperatures due to the topological defects.
Southern and Xu[143] studying by MC simulations the vorticity associated to the vortex–antivortex proposed that the vorticity has a jump at the critical temperature similar to that of the KT transition.
Kawamura and Kikuchi[145] using different boundary conditions in MC simulations also observed various phenomena associated to the vorticity which, according to them, are a proof of a phase transition.
Last, Wintel et al.[146] have studied theoretically and numerically the region above the suspected critical temperature for the triangular antiferromagnetic lattice ($T_c \sim 0.29$). They claimed that the correlation length and susceptibility must follow a KT law.

There are numerical evidences of the importance of topological defects at finite temperatures and it seems that these systems undergo a kind a topological phase transition. Nevertheless we have no certainties that the phenomena present at finite sizes would hold for the infinite size.

5.7. *Frustrated Heisenberg spin systems: $Z_2 \otimes SO(3)$, $Z_3 \otimes SO(3)$ ...*

By inspecting Table 3 it is not difficult to see that other order parameters exist in frustrated systems. One of the most interesting should be $Z_2 \otimes SO(3)$. It corresponds to a non planar GS which could exist in experimental systems. Numerically the simplest system would be the Stiefel $V_{3,3}$ model or equivalently the Ising–$V_{2,2}$ model. The comparison with the XY case would be very interesting. In particular the Ising transition could appear near the $SO(3)$ transition (see previous section) and the coupling between the Z_2 walls and the vortex could be very instructive. If we follow the second hypothesis of Olsson for the XY case (see section 5.3), the transition should display an "almost second-order transition".

Symmetrically the coupling of the $SO(3)$ vortex with a Z_3 Potts model which appear in the Potts–$V_{3,2}$ model could also disclose interesting properties. Does it show first-order properties as for $SO(2)$ vortex?

Some other breakdowns of symmetry could also appear like $Z_3 \otimes Z_2 \otimes SO(3)$ in the antiferromagnetic triangular lattice with large NNN interaction. Similar questions appear. We note that the $SO(3)/SO(2)$ order parameter does not have a topological transition. The transition of the type $Z_2 \otimes SO(3)/SO(2)$ for the J_1–J_2 model or $Z_3 \otimes SO(3)/SO(2)$ for the triangular lattice with intermediate NNN interaction should have a standard transition (Ising or three-state Potts model).

5.8. *Topological defects for $N \geq 4$*

Some other topological defects should exist for an order parameter of the type $SO(N)$, with a GS in $N-1$ dimensions, $Z_2 \otimes SO(N)$, with a GS in N dimensions, and $Z_q \otimes SO(N)$ with a coupling of a GS in $N-1$ dimensions and a lattice symmetry $\cdots$ All questions raised for Heisenberg spins still hold in these cases.

6. General conclusions

In this chapter we have studied the phase transition in frustrated systems between two and four dimensions. We have found various breakdowns of symmetry, contrary to the unique one for ferromagnetic systems.

In three dimensions the transition is always of first order in the thermodynamic limit. However for "small" sizes in numerical simulations or for temperatures not "too close" to the transition temperatures in experiments, the system could display an "almost universality class" for an

$O(N)/O(N-2)$ breakdown of symmetry. Many compounds studied experimentally are in this class.

In two dimensions the situation is much less clear. Indeed the topological defects can play a fundamental role and their couplings with a discrete symmetry (Ising or Potts) is unknown. We hope that in the near future the two-dimensional case will be clarified as the three-dimensional one on which our understanding has increased considerably in the last decade.

Acknowledgments

I am grateful to Prof. K. D. Schotte and Sonoe Sato for their support, discussions, and for critical reading of the manuscript. This work was supported by the DFG SCHO 158/10-1.

Appendix A: Monte Carlo Simulation

The purpose of this section is just to show the fastest algorithm to run Monte Carlo simulations, the best method to distinguish a first-order transition from a second-order one and to extract the critical exponents with a reliable estimate of errors.

Markov chains and algorithms: Since we cannot enumerate all the spin configurations, we are forced to use numerical simulations to calculate the physical quantities. The method of choice is the Monte Carlo method generating a set of phase–space configurations from a Markov chain defined by the transition probability $W[s, s']$ between states $\{s\}$ and $\{s'\}$, where the new configuration depends only on the preceding one. There are many ways to get the transition probability $W[s, s']$.[147] The Metropolis algorithm is the simplest but not very efficient one. A new heat–bath algorithm, called Fast Linear Algorithm,[140] for vector spins is more efficient. For example it is three times faster than the Metropolis algorithm for a two-dimensional triangular antiferromagnetic lattice at the critical temperature. Furthermore the use of the over–relaxation[147] can reduce strongly the autocorrelation time.[111] The cluster algorithm cannot be used for frustrated spin systems. Indeed there are two problems. The first is to take into account the competition of different interactions in a plaquette. It means that many spins should be considered in one step when constructing the cluster. Second, even if we were able to construct a cluster, the BS is no more $O(N)/O(N-1)$, but $O(N)/O(N-2)$, for example. Consequently a symmetry to a $N-1$ plane used in the Wolff's algorithm[148] should be changed.

Thermodynamic averages are taken simply by

$$\bar{A} \;=\; (1/N_{MC}) \sum_{t=1}^{N_{MC}} A[t] \tag{9}$$

where N_{MC} is the number of new configurations generated (Monte Carlo Steps) and $A[t]$ the value of the quantity at step t. The great advantage of this method is that the partition function $Z = \sum_{\{s\}} e^{-\beta E[s]}$ needs not be calculated.

To estimate the errors of the averaged quantities we have to take into account that each new configuration is correlated with the previous one. We define the autocorrelation time τ by the number of MC steps required to obtain two uncorrelated spin configurations. It is calculated using the autocorrelation function[149] $C(t) = (1/\chi)[\langle A(t)A(0)\rangle - \langle A\rangle^2]$ where time is measured in MC steps (see comments in the appendix of Ref. [22]). If $N \gg \tau$, then a useful approximation for the error in $\bar{A}$ is given by

$$(\delta\bar{A})^2 = \frac{\chi}{N_{MC}/(1+2\tau)} \tag{10}$$

$$\chi = \langle A^2\rangle - \langle A\rangle^2 . \tag{11}$$

This expression is identical to the standard deviation but with an effective number of independent measurements given by

$$\frac{N_{MC}}{1+2\tau}. \tag{12}$$

Problems arise when quantities are a combination of different averages, for example the susceptibility (11). We could try to treat $\langle A^2\rangle$ and $\langle A\rangle^2$ as independent quantities and estimate the error by the sum of the errors of the two quantities. But the result will be overestimated due to the correlation between the two elements of the sum. To solve this problem we can use, for example, the Jackknife procedure.[150] An application of this method can be found in the appendix of Ref. [22].

The histogram method: The great advantage of the histogram method in the analysis of MC data is that a run at a single temperature T_1 can be used to extract results for a continuous range of nearby temperatures.[151] In practice the range of temperature over which $\langle A\rangle$ may be estimated from a single MC run at T_1 is limited by the range over which reliable statistics can be expected for $H(E)$, the histogram of the energy. A rough guide is $T_a < T < T_b$, where T_a and T_b correspond to the energies

$\langle E_a \rangle$ and $\langle E_b \rangle$ at which $H(E) \simeq \frac{1}{2} H_{max}$. Since $H(E)$ becomes more sharply peaked with system size, the valid temperature range becomes smaller as L increases. Multiple histograms made at a number of nearby temperatures may be combined to increase accuracy.

Nature of the transition: Differentiating a weak first-order from a second-order transition could be difficult. The finite size scaling (FSS) for a first-order transition has been extensively studied .[152,153,154] A first-order transition should be identified by the following properties:

a) The histogram of the energy, $P_T(E)$, has a double peak.
b) The minimum of the fourth order energy cumulant W varies as: $W = W^* + b\, L^{-d}$ where W^* is different from $2/3$.
c) The temperatures $T(L)$ at which the specific heat C or the susceptibility χ has a maximum should vary as $T(L) = T_c + a\, L^{-d}$.
d) The maximum of C and χ are proportional to the volume L^d.

Obviously a double peak of $P_T(E)$ which becomes more pronounced when the size increases is preferable (way a). If the two peaks are too close, the three other possibilities (b, c and d) can check if the probability is gaussian (second-order transition) or not (first-order transition) in the limit of infinite size.

Second-order phase transition: For a second-order phase transition the interesting parameters are the critical temperature and the critical exponents. There are at least three main ways to calculate them:

a) Consider the high and low temperature regions where the correlation length $\xi \ll L$. There, we can fit $\xi = a_\xi (T - T_c)^{-\nu} +$corrections. The corrections become less important near T_c, but then ξ is very large, and a very big system size is necessary. Furthermore the autocorrelation time $\tau \sim (T - T_c)^{-z}$ becomes also very large and the error $\delta\xi$ becomes very big even if we can use some tricks to diminish it.[155]
b) The Finite Size Scaling (FSS) region is the most powerful method. It is the region with ξ(theoretical) $\gg L$. The best method is to calculate the Binder cumulant[156] $U_L(T) = 1 - \frac{\langle M^4 \rangle}{3 \langle M^2 \rangle^2}$ for different size L.
1. We can calculate the critical exponents directly by plotting $\chi L^{-\gamma/\nu}$ as a function of $U_L(T)$ and all the curves must collapse

for the correct exponent $-\gamma/\nu = \eta - 2$.[157] Indeed we can write $\chi L^{\eta-2} = h(U_L)$ with h an unknown function. The other exponents β/ν and ν can be obtained similarly using the magnetization and $V_1 = \frac{\langle ME\rangle}{\langle M\rangle} - \langle E\rangle$. It is the fastest way to get the critical exponents. This method works well even for the Kosterlitz-Thouless transition.[158]

2. We can also use $U_L(T)$ to calculate the critical temperature T_c using the crossing of U_L for different sizes. Very good statistics is needed because the evaluation of the first correction is necessary to get a correct value of T_c.

3. Having determined T_c we can calculate the critical exponents using, for example, $\chi \propto L^{+\gamma/\nu}, \cdots$

4. The last properties are also valid for the maximum (or minimum) of χ and V_1, but we need many simulations at various temperatures to find the maxima because their locations vary as a function of the size L and are different for each quantity.

c) The dynamical properties[159,160,161,162,163] are not very often used even if it is surely the fastest method available. One has to prepare a state in the GS (i.e. $T = 0$) or randomly (i.e. $T = \infty$), and to observe the dynamical properties of the system at the critical temperature $T = T_c$ for a finite number of Monte Carlo steps before the equilibrium is reached. For an example see Ref. [111].

Kosterlitz–Thouless (KT) transition: A KT transition [106] exists for two-dimensional lattices with XY spins. The unbounding of vortex–antivortex pairs appear at the critical temperature, $T_c \sim 0.9$ for square lattice.

This transition has some special features: for $T < T_c$ the correlation length (ξ) is infinite, while for $T > T_c$ it has an exponential decreasing contrary to the power law behavior in the standard transition.

To find T_c and the critical exponents we have several ways:

a) we can fit ξ in the high temperature region, which is problematic because of the many free parameters and of the exponential form.

b) we can use a method using the behavior of various quantities in the finite size scaling region (FSS) where $\xi \gg L$.

1. The first one is to use the universal jump of the helicity Υ at the critical temperature (in the finite size scaling region where $\xi \gg L$), but this method requires the jump of $\Upsilon(L)$ which is known for the

non frustrated case, but not for the frustrated case.
2. It is therefore interesting to find another method to get the critical exponent, even without calculating T_c. The method (b.1.) introduced previously for a second-order phase transition using the Binder parameter works well for the KT transition.[158] The Binder parameter, contrary to the common belief, crossed around T_c. Plotting $\chi L^{\eta-2}$ as a function of U_L for various sizes, the curves collapse at the correct value of $\eta = 0.25$. This method can be applied whatever the form of ξ is. Therefore it should be applicable to all phase transitions.

c) The dynamical behavior of this system can also be used .[162]

For the two-dimensional ferromagnetic XY spin system, all methods mentioned above are in agreement.

Appendix B: Renormalization Group: Landau-Ginzburg theory, expansions in fixed dimension $d = 3$ and for $d = 4 - \epsilon$ and its implications for experiments

In this short section we would like to give the necessary knowledge to help to understand the concepts of fixed points, flow diagrams and crossovers.

First consider a system of Heisenberg spins with a Hamiltonian:

$$H = -J_1 \sum_{(ij)} \mathbf{S}_i.\mathbf{S}_j \,, \tag{13}$$

and the spin is restricted to be of norm $S = 1$. Replacing this constraint by an exponential potential $S = 1 \Leftrightarrow \int_0^\infty e^{u(\mathbf{S}^2-1)^2} \cdot dS$ the Hamiltonian can be written in the form

$$H = K \sum_{<ij>} (\mathbf{S}(i) - \mathbf{S}(j))^2 + r \sum_i \mathbf{S}(i)^2 + u_0 \sum_i \left(\mathbf{S}(i)^2\right)^2 \,. \tag{14}$$

Two remarks:
1. Other terms could be added in the Hamiltonian. These additional terms could be unimportant that means they become irrelevant near the fixed point (see later). Or we cannot treat them, that means they are not renormalizable in technical terms. If these neglected terms are important the method cannot describe the physics of the phase transition. This unfortunate case occurs for frustrated system for low dimensions of space and spins.[32]
2. In addition, since the transformation is not exact, the starting value u_0 cannot be known even if it is possible to make a rough guess.[32]

We have plotted in the Fig. 13 the RG flow for this model.

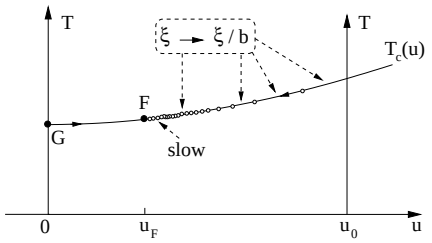

Fig. 13. RG flow for (14). F is the stable fixed point, G is the Gaussian one. Near F the flow is very slow.

The system will physically keep its value u_0. But its RG flow will not. Following a series of steps the value of u will change in approaching the fixed point F. At each step the correlation length of the system will be divided by a factor $b > 1$. In addition the flow becomes slower near the fixed point F. Consequently, to reach the neighborhood of F, where the system have a second-order transition, the initial ξ must be large "enough". We know that $\xi(T) \sim (T - T_c)^{-\nu}$ for a second-order phase transition. Hence, to obtain numerically or experimentally ξ which follows a power law (without too many corrections), the temperature must be close "enough" to the critical temperature T_c. Numerically, in the Finite Size Scaling (FSS) regions where ξ(theoretical is much bigger than the size of the system L, the FSS law (see 6) will be valid only for L large "enough". We observe that in the Fig. 9 only the plane $T_c(u, v)$ is plotted.

Consider now a model with a XY anisotropy, for example we add to the Hamiltonian (13) a term $D \sum_i (S_i^z)^2$ with $0 < D \ll 1$. We have now two parameters in our Landau-Ginzburg model: u for the length of the spin and v associated to D. The critical plane (u, v) of the flow diagram of this model is plotted in Fig. 14. From the initial point $(u_0, v_0 \ll 1)$ the flow will go close to the Heisenberg fixed point F_H and then has a crossover to the F_{XY} fixed point. Near F_H the flow is very slow and needs a lot of steps to escape from the influence of F_H and reaches finally the neighborhood of F_{XY}. Therefore, to observe the "true" XY behavior, the correlation length must be very large. That means that the temperature must be very close of T_c or, if we are in the FSS region, the system size must be very large.

We must know the stability of the fixed point when anisotropies are present. The "quasi" general rule is that the system goes to the fixed

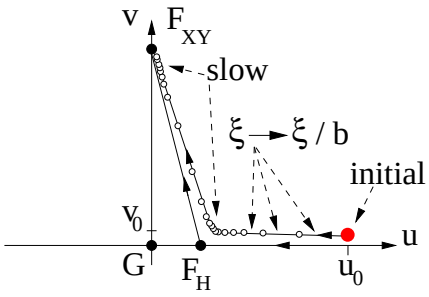

Fig. 14. Schematic RG flow ($T_c(u,v)$ plane) for (14 with $D\sum_i (S_i^z)^2$). F_H is the Heisenberg fixed point, F_{XY} is the XY fixed point, G is the Gaussian one. Near F_H and F_{XY} the flow is very slow.

point with the lowest spin symmetry and the biggest space dimensions. For example consider the quasi one-dimensional system $CsMnBr_3$. This compound will display a one-dimensional behavior before reaching the three-dimensional behavior. Another example is $Cu(HCOO)_2 2CO(ND_2)_2 2D_2O$ which has a small Ising anisotropy. In this case the system will show a Heisenberg behavior before showing the Ising behavior. In real compounds small "anisotropies" are almost always present. Therefore many crossovers will appear when the temperature approaches the critical temperature. Consequently interpretations of experiments could be difficult.

To get the critical exponent and the flow diagram, the expansion in fixed dimension d or in $d = 4 - \epsilon$ consists of expanding the exponential $e^{Hamiltonian(u)}$ around the Gaussian fixed point $u = 0$. Results are in the form of a power series of u. Unfortunately this series is not convergent, but in the ferromagnetic case it has been shown to be resummable with Pade–Borel techniques. However, there are many ways to resum and one must be chosen following some criteria.[87] This resummation has been proved efficient for ferromagnetic systems, however it is not certain that it will work for frustrated systems. Indeed the presence of two vectors ($O(N)/O(N-2)$ BS in this case (compared to the $O(N)/O(N-1)$ BS in the ferromagnetic case) gives rise to a series of power of u and v (u,v, uv, u^2, $\cdots$) and this double expansion is difficult to resum.

References

1. T. Inui, Y. Tanabe, Y. Onodera, *Group Theory and its Applications in Physics*, Springer Series in Solid–State–Sciences 78, Berlin 1990
2. S.A. Antonenko, A.I. Sokolov, Phys. Rev. E **51**, 1894 (1995)

3. G. Toulouse, Commun. Phys. **2**, 115 (1977)
4. J. Villain, J. Phys. C **10**, 1717 (1977)
5. H. Kawamura, J. Phys. Soc. Jpn. **61**, 1299 (1992), **58**, 584 (1989), **56**,474 (1987), **55**, 2095 (1986)
6. M.L. Plumer and A. Mailhot, Phys. Rev. B **50**, 16113 (1994)
7. E. H. Boubcheur, D. Loison, and H.T. Diep, Phys. Rev. B **54**, 4165 (1996)
8. M. Itakura, J. Phys. Soc. Jpn **72**, 74 (2003)
9. M.L. Plumer and A. Mailhot, J. Phys: Condens. Matter. **9**, L165 (1997)
10. M.L. Plumer and A. Mailhot, Phys. Rev. B **50**, 6854 (1994)
11. D. Loison and H.T. Diep, Phys. Rev. B **50**, 16453 (1994)
12. T. Bhattacharya, A. Billoire, R. Lacaze and Th. Jolicoeur, J. Phys. I (Paris) **4**, 181 (1994)
13. D. Loison, A.I. Sokolov, B. Delamotte, S.A. Antonenko, K.D. Schotte and H.T. Diep, JETP Letters **76**,337 (2000)
14. Th. Jolicoeur, E. Dagotto, E. Gagliano, and S. Bacci, Phys. Rev. B **42**, 4800 (1990)
15. C.L. Henley, J. Appl. Phys. **61**, 3962 (1987). Also see: M.T. Heinilä and A.S. Oja, Phys. Rev. B **48**, 7227 (1993)
16. J. Villain, R. Bidaux, J.-P. Carton, and R. Conte, J. Phys. (Paris) **41**, 1263 (1980)
17. W. M. Saslow, M. Gabay, and W.M. Zhang, Phys. Rev. L **68**, 3627 (1992)
18. H. Kawamura, Prog. Theo. Phys. Suppl. **101**, 545 (1990), W.-M. Zhang, W.M. Saslow, M. Gabay, Phys. Rev. B **44**, 5129 (1991),0204 (1993)
19. H.T. Diep, Europhys. Lett. **7**, 725 (1988), Phys. Rev. B **39**, 397 (1989)
20. D. Loison, Physica A **275**, 207 (1999)
21. R. Quartu and H.T. Diep, J. Magn. and Magn. Mater. **182**, 38 (1998)
22. D. Loison and P. Simon, Phys. Rev. B **61**, 6114 (2000)
23. H.T. Diep, A. Ghazali, and P. Lallemand, J. Phys. C **18**, 5881 (1985)
24. P. Lallemand, H.T. Diep, A. Ghazali, and G. Toulouse, J. Physique-Lettres **468**, 1087 (1985)
25. J.L. Alonso et al., Phys. Rev. B **53**, 2537 (1996)
26. C. Pinettes and H.T. Diep, Journal of Applied Physics, **83**,6317 (1998)
27. A. Moreo, E. Dagotto, T. Jolicoeur, and J. Riera, Phys. Rev. B **42**, 6283 (1990), J. Ferrer, Phys. Rev. B **47**, 8769 (1993)
28. H.T. Diep and H. Kawamura, Phys. Rev. B **40**, 7019 (1989)
29. H.T. Diep, Phys. Rev. B **45**, 2863 (1992)
30. J.N. Reimers, Phys. Rev. B **45**, 7295 (1992), A. Mailhot and M. L. Plumer, Phys. Rev. B **48**, 9881 (1993), S.T. Bramwell, M.J.P. Gingras, and J.N. Reimers, J. Appl. Phys. **75**, 5523 (1994)
31. E.H. Boubcheur, R. Quartu, H.T. Diep, and O. Nagai, Phys. Rev. B **58**, 400 (1998)
32. See the chapter of B. Delamotte, D. Mouhanna, and M. Tissier in this book
33. A. Dobry and H.T. Diep, Phys. Rev. B **51**, 6731 (1995)
34. D. Loison and K.D. Schotte, Eur. Phys. J. B **5**, 735 (1998)
35. D. Loison and K.D. Schotte, Eur. Phys. J. B **14**, 125 (2000)
36. D. Loison and K.D. Schotte, Submitted to Eur. Phys. J. B

37. H. Kunz and G. Zumbach,J. Phys. A **26**, 3121 (1993)
38. H.T. Diep and D. Loison, J. Appl. Phys. **76**, 6350 (1994)
39. D. Loison, Eur. Phys. J. B **15**, 517 (2000)
40. D. Loison, not published.
41. D. Loison, Phys. Lett. A **257**, 83 (1999), Phys. Lett. A **264**, 208 (1999)
42. R.J. Baxter, J. Phys. C **6**, L445 (1973); *Exactly solved models in statistical mechanics* (Academic Press, London, 1982)
43. P. Peczak and D.P. Landau, Phys. Rev. B **39**, 11932 (1989)
44. D. Loison, submitted to Euro. J. Phys. B.
45. G. Zumbach, Nucl. Phys. B **413**, 771 (1994), Phys. Lett. A **190**, 225 (1994), Phys. Rev. Lett. **71**, 2421 (1993)
46. A.Z. Patashinskii and V.I. Pokrovskii, *Fluctuation Theory of Phase Transitions*, (Pergamon press 1979), §VII, **6**, *The S-matrix method and unitary relations*
47. J. Zinn-Justin, *Quantum Field Theory and Critical Phenomena*, (Oxford University Press, Oxford, 1996), §7.4 *Real-time quantum field theory and S-matrix*, §11.8 *Dimensional regularization, minimal subtraction: calculation of RG functions*
48. M. Tissier, D. Mouhanna, and B. Delamotte, Phys. Rev. B **61**, 15327 (2000), ibid **67**, 134422 (2003)
49. T.E. Mason, Y.S. Yang, M.F. Collins, B.D. Gaulin, K.N. Clausen and A. Harrison, J. Magn. and Magn. Mater **104-107**, 197 (1992)
50. T.E. Mason, M.F. Collins and B.D. Gaulin, J. Phys. C **20**, L945 (1987)
51. Y. Ajiro, T. Nakashima, Y. Unno, H. Kadowaki, M. Mekata and N. Achiwa, J. Phys. Soc. Japan **57**, 2648 (1988)
52. B.D. Gaulin, T.E. Mason, M.F. Collins and J.F. Larese, Phys. Rev. Lett. **62**, 1380 (1989)
53. T.E. Mason, B.D. Gaulin and M.F. Collins, Phys. Rev. B **39**, 586 (1989)
54. H. Kadowaki, S.M. Shapiro, T. Inami and Y. Ajiro, J. Phys. Soc. Japan **57**, 2640 (1988)
55. J. Wang, D.P. Belanger and B.D. Gaulin, Phys. Rev. Lett. **66**, 3195 (1991)
56. H. Weber, D. Beckmann, J. Wosnitza, H.v. Löhneysen and D. Visser, Inter. J. Modern Phys. B **9**, 1387 (1995)
57. T. Goto, T. Inami and Y. Ajiro, J. Phys. Soc. Japan **59**, 2328 (1990)
58. R. Deutschmann, H.v. Löhneysen, J. Wosnitza, R.K. Kremer and D. Visser, Euro. Phys. Lett, **17**, 637 (1992)
59. M.F. Collins, O.A. Petrenko, Can. J. Phys. **75**, 605 (1997)
60. T. Kato, T. Asano, Y. Ajiro, S. Kawano, T. Ihii and K. Iio Physica B **213-214**, 182 (1995)
61. T. Kato, K. Iio, T. Hoshimo, T. Mitsui and H. Tanaka, J. Phys. Soc. Japan **61**, 275 (1992)
62. H. Tanaka, H. Nakamo and S. Matsumo, J. Phys. Soc. Japan **63**, 3169 (1994)
63. H. B. Weber, T. Werner, J. Wosnitza H.v. Löhneysen and U. Schotte, Phys. Rev. B **54**, 15924 (1996)
64. D.A. Tindall, M.O. Steinitz and M.L. Plumer, J. Phys. F **7**, L263 (1977)
65. K.D. Jayasuriya, S.J. Campbell and A.M. Stewart, J. Phys. F **15**, 225 (1985)

66. B.D. Gaulin, M. Hagen and H.R. Child, J. Physique Coll. **49** C8, 327 (1988)
67. T.R. Thurston, G. Helgesen, D. Gibbs, J.P. Hill, B.D. Gaulin and G. Shirane, Phys. Rev. Lett. **70**, 3151 (1993) , T.R. Thurston, G. Helgesen,J.P. Hill, D. Gibbs, B.D. Gaulin and P.J. Simpson, Phys. Rev. B **49**, 15730 (1994)
68. P. Du Plessis, A.M. Venter and G.H.F. Brits J. Phys. (Cond. Mat.) **7**, 9863 (1995)
69. J. Ecker and G. Shirane, Solid State Commun. **19**, 911 (1976)
70. G. Helgesen, J.P. Hill, T.R. Thurston, D. Gibbs, J. Kwo and M. Hong, Phys. Rev. B **50**, 2990 (1994)
71. S.W. Zochowski, D.A. Tindall, M. Kahrizi, J. Genosser and M.O. Steinitz, J. Magn. Magn. Mater. **54-57**, 707 (1986)
72. H.U. Åström and G. Benediktson, J. Phys. F **18**, 2113 (1988)
73. F.L. Lederman and M.B. Salomon, Solid State Commun. **15**, 1373 (1974)
74. K.D. Jayasuriya, S.J. Campbell and A.M. Stewart, Phys. Rev B **31**, 6032 (1985)
75. P. Du Plessis, C.F. Van Doorn and D.C. Van Delden, J. Magn. Magn. Mater. **40**, 91 (1983)
76. G.H.F. Brits and P. Du Plessis, J. Phys. F **18**, 2659 (1988)
77. E. Loh, C.L. Chien and J.C. Walker, Phys. Lett. **49A**, 357 (1974)
78. K.D. Jayasuriya, A.M. Stewart, S.J. Campbell and E.S.R. Gopal, J. Phys. F **14**, 1725 (1984)
79. O.W. Dietrich and J. Als-Nielsen, Phys. Rev. **162**, 315 (1967)
80. C.C. Tang, P.W. Haycock, W.G. Stirling, C.C. Wilson, D. Keen, and D. Fort, Physica B **205**, 105 (1995)
81. K.H. Hirota, G. Shirane, P.M. Gehring and C.F. Majkrzak, Phys. Rev B **49**, 11 967 (1994), P.M. Gehring, K.H. Hirota,C.F. Majkrzak and G. Shirane, Phys. Rev L **71**, 1087 (1993)
82. C.C. Tang, W.G. Stirling, D.L. Jones, A.J. Rolloson, A.H. Thomas and D. Fort, J. Magn. Magn. Mater. **103**, 86 (1992)
83. H. Kadowaki, K. Ubukoshi, K. Hirakawa, J.L. Martinez and G. Shirane, J. Phys. Soc. Japan **56**, 4027 (1987)
84. J. Wosnitza, R. Deutschmann, H.v Löhneysen and R.K. Kremer, J. Phys.: Condens. Matter **6**, 8045 (1994)
85. K. Koyama and M. Matsuura, J. Phys. Soc. Japan **54**, 4085 (1985)
86. G.C. DeFotis, F. Palacio and R.L. Carlin, Physica B **95**, 380 (1978), G.C. DeFotis and S.A. Pugh, Phys. Rev. B **24**, 6497 (1981), G.C. DeFotis and J.R. Laughlin, J. Magn. Magn. Mater. **54-57**, 713 (1986)
87. J.C. Le Guillou and J. Zinn-Justin, J. Phys. (Paris) Lett. **46**, L137 (1985)
88. S.A. Antonenko, A.I. Sokolov and V.B. Varnashev, Phys. Lett. A **208**, 161 (1995)
89. B. Kastening, Phys. Rev. D **57**, 3567 (1998)
90. S.A. Antonenko and A.I. Sokolov, Phys. Rev. B **49**, 15901 (1994)
91. A. Pelisseto, P. Rossi, and E. Vicari, Phys. Rev. B **63**, 140414(R)(2001)
92. P. Calabrese, P. Parruccini, and A.I. Sokolov, Phys. Rev. B **66**, 180403(R) (2002)

93. P. Azaria, B. Delamotte,F. Delduc and T. Jolicoeur, Nucl. Phys. B **408**, 485 (1993), P. Azaria, B. Delamotte and T. Jolicoeur, Phys. Rev. Lett. **64**, 3175 (1990), J. App. Phys. **69**, 6170 (1991)
94. B.W. Southern and A.P. Young, Phys. Rev. B **48**, 13170 (1993)
95. D.R.T. Jones, A. Love, and M.A. Moore, J. Phys. C **9**, 743 (1976)
96. B. Nienhuis, A.N. Berker, E.K. Riedel, and M. Schick, Phys. Rev. Lett. **43**, 737 (1979)
97. M. Nauenberg and B. Nienhuis, Phys. Rev. Lett. **33**, 944 (1974)
98. L. Saul, Phys. Rev. B **46**, 13847 (1992)
99. H. Kawamura, J. Phys. Soc. Jpn **59**, 2305 (1990)
100. N.D. Mermin and H. Wagner, Phys. Rev. Lett. **17**, 1133 (1966)
101. N.D. Mermin, Rev. Mod. Phys. **51**, 591 (1979)
102. G. Toulouse and M. Kleman, J. Physique Lett. **37**, 149 (1976)
103. G. Kohring, R. E. Shrock, and P. Wills, Phys. Rev. Lett. **57**, 1358 (1986)
104. G. A. Williams, Phys. Rev. Lett. **59**, 1926 (1987)
105. S. R. Shenoy and B. Chattopadhyay, Phys. Rev. B **51**, 9129 (1995), Phys. Rev. Lett. **72**, 400 (1994), B. Chattopadhyay, M. C. Mahato, and S. R. Shenoy, Phys. Rev. B **47**, 15159 (1993), S. R. Shenoy, Phys. Rev. B **42**, 8595 (1990), Phys. Rev. B **40**, 5056 (1989)
106. V.L. Berezinskii, Soviet Physics JETP **32**, 493 (1971), J.M. Kosterlitz and D.J. Thouless, J. Phys. C **6**, 1181 (1973), J.M. Kosterlitz, J. Phys. C **7**, 1046 (1974)
107. J. Lee, J.M. Kosterlitz, and E. Granato, Phys. Rev. B **43**, 11531 (1991)
108. S. Miyashita and H. Shiba, J. Phys. Soc. Jpn **53**, 1145 (1984)
109. S. Lee and K.C. Lee, Phys. Rev. B **57**, 8472 (1998)
110. L. Caprioti, R. Vaia, A. Cuccoli, and V. Togneti, Phys. Rev. B **58**, 273 (1998)
111. D. Loison, cond-mat/0001122, unpublished
112. S. Teitel and C. Jayaprakash, Phys. Rev. Lett. **51**, 1999 (1983); Phys. Rev. B **27**, 598 (1983)
113. B. Berge, H.T. Diep, A. Ghazali, and P. Lallemand, Phys. Rev. B **34**, 3177 (1986)
114. D.B. Nicolaides, J. Phys. A **24**, L231 (1991)
115. J.V. Jose and G. Ramirez-Santiago, Phys. Rev. Lett. **77**, 4849 (1996); **68**, 1224 (1992); Phys. Rev. B **49**, 9567 (1994)
116. J.M. Thjissen and H.J.F. Knops, Phys. Rev. B **42**, 2438 (1990)
117. E. Granato, M.P. Nightingale, Phys. Rev. B **48**, 7438 (1993)
118. S. Lee and K.C. Lee, Phys. Rev. B **49**, 15184 (1994)
119. H.J. Luo, L. Schülke, and B. Zheng, Phys. Rev. Lett. **81**, 180 (1998)
120. M. Benakly and E. Granato, Phys. Rev. B **55**, 8361 (1997)
121. M.P. Nightingale, E. Granato, and J.M. Kosterlitz, Phys. Rev. B **52**, 7402 (1995).
122. J. Lee, E. Granato, and J.M. Kosterlitz, Phys. Rev. Lett. **66**, 2090 (1991); Phys. Rev. B **44**, 4819 (1991).
123. P. Olsson, Phys. Rev. Lett. **75**, 2758 (1995); **77**, 4850 (1996); Phys. Rev. B **55**, 3585 (1997)

124. Y.M.M. Knops, B. Nienhuis, H.J.F. Knops, and J.W. Blöte, Phys. Rev. B **50**, 1061 (1994)
125. E. Granato, Phys. Rev. B **45**, 2557 (1992)
126. M. Yosefin and E. Domany, Phys. Rev. **B 32**, 1778 (1985)
127. P. Minnhagen, Phys. Rev. Lett **54**, 2351 (1985); Phys. Rev. B **32**, 3088 (1985)
128. G.S. Grest, Phys. Rev. B **39**, 9267 (1989)
129. J.R. Lee, Phys. Rev. B **49**, 3317 (1994)
130. M.Y. Choi and D. Stoud, Phys. Rev. B **32**, 5773 (1985)
131. G.S. Jeon, S.Y. Park, and M.Y. Choi, Phys. Rev. B **55**, 14088 (1997)
132. S. Lee, K.C. Lee, and J.M. Kosterlitz cond-mat/9612242 (unpublished)
133. C.J. Lobb, Physica B **152**, 1 (1988)
134. X.S. Ling, H.J. Lezec, J.S. Tsai, J. Fujita, H. Numata, Y. Nakamura, Y. Ochiai, Chao Tang, P.M. Chaikin, and S. Bhattacharya, Phys. Rev. Lett. **76**, 2989 (1996)
135. T.C. Halsey, J. Phys. C **18**, 2437 (1985)
136. S.E. Korshunov, J. Stat. Phys. **43**, 17 (1986)
137. V. Kotsubo, K.D. Hahn, and J.P. Parpia, Phys. Rev. Lett. **58**, 804 (1987)
138. J. Xu and C. Crooker, Phys. Rev. Lett. **65**, 3005 (1990)
139. T. Garel and S. Doniach, J. Phys. C **13**, L887 (1980)
140. The Fast Linear Algorithm developped by D. Loison is three times faster than the Metropolis algorithm at the critical temperature for frustrated two dimensional systems. Submitted to Euro. J. Phys. B. Accessible at the home page `http://www.physik.fu-berlin.de/~loison/`
141. D. Loison, submitted to Euro. J. Phys. B.
142. H. Kawamura and S. Miyashita, J. Phys. Soc. Jpn **53**, 1145 (1985)
143. M. Caffarel, P. Azaria, B. Delamotte, and D. Mouhanna, Phys. Rev. B **64**, 014412 (2001)
144. B.W. Southern and H.J. Xu, Phys. Rev. B **52**, R3836 (1995)
145. H. Kawamura and M. Kikuchi, Phys. Rev. B **47**, 1134 (1993)
146. M. Wintel, H.U. Everts and W. Apel, Europhys. Lett **25**, 711 (1994), Phys. Rev. B **52**, 13480 (1995)
147. M. Creutz, Phys. rev. B **36**, 515 (1987)
148. U. Wolff, Phys. Rev. Lett. **62**, 361 (1989), Nucl. Phys. B **322**, 759 (1989)
149. H. Müller-Krumbhaar and K. Binder, J. Stat. Phys. **8**, 1 (1973)
150. B. Efron, *The Jackknife, The Bootstrap and other Resampling Plans* (SIAM, Philadelphia, PA, 1982)
151. A.M. Ferrenberg and R.H. Swendsen, Phys. Rev. Lett. **61**, (1988) 2635; *ibid* **63**, (1989) 1195; Computers in Physics, Sept/Oct (1989) 101
152. V. Privman and M.E. Fisher, J. Stat. Phys. **33**, 385 (1983)
153. K. Binder, Rep. Prog. Phys. **50**, 783 (1987)
154. A. Billoire, R Lacaze and A. Morel, Nucl. Phys. B **370**, 773 (1992)
155. G. Prussner, D. Loison and K.D. Schotte, Physica A **299**, 557 (2001)
156. K. Binder, Z. Phys. B **43**, 119 (1981)
157. D. Loison, Physica A **271**, 157 (1991)
158. D. Loison, J. Phys.: Condens. Matter, **11**, L401 (1999)

159. Z. Phys. B **73**, 539 (1989)
160. D.A. Huse, Phys. Rev. B **40**, 304 (1989)
161. K. Humayun and A.J. Bray, J. Phys. A **24**, 1915 (1991)
162. B. Zhang, Int. J. Mod. Phys. **12**, 1419 (1998)
163. H.J. Luo and B. Zheng, Mod. Phys. Lett. B **11**, 615 (1997)